Master's thesis

Elisabeth Nordnes

Softening and Melting Properties of Quartz

Master's thesis in Chemical Engineering and Biotechnology
Supervisor: Halvard Tveit
June 2019

NTNU
Norwegian University of
Science and Technology

Elisabeth Nordnes

Softening and Melting Properties of Quartz

NTNU
Norwegian University of
Science and Technology

Preface

This report is the evaluation basis for the course TMT4900 Materials Chemistry and Energy Technology, Master´s Thesis, submitted to the Norwegian University of Science and Technology (NTNU). It is a part of the collaborative project High Temp Quartz, with an aim to investigate and identify how and in what way different quartz properties are affecting the silicon furnace. This master´s thesis describes an investigation of the effect of quartz type on softening and melting properties of quartz, and in what way it affects the furnace. To measure softening and melting temperature of three different quartz types, a sessile drop furnace was used. The phase composition of the different quartzes was detected with XRD, after heat treatment to a temperature right below the softening temperature in a rapid heating furnace. To achieve a better understanding of heat transfer and temperature distribution in quartz, the software COMSOL Multiphysics was used. All results were used to evaluate the effect in a real furnace. The project was done in collaboration with Elkem ASA and SINTEF. The experiments were performed at the Department of Materials Science and Engineering at NTNU.

I would like to thank my supervisors, Prof. II Halvard Tveit at NTNU and Senior Research Scientist Eli Ringdalen at SINTEF, for giving me the opportunity to write this project, and for helpful discussions and feedback. I would also like to thank Sarina Bao (SINTEF) for help with the sessile drop furnace, Julian Tolchard (SINTEF) for performing the XRD analysis, Karin Fjeldstad Jusnes (NTNU) and Berit Kramer (NTNU) for help and training with the rapid heating furnace, and Edin Myrhaug for help with modeling in COMSOL.

Trondheim, June 2019

Elisabeth Nordnes

Abstract

This master´s thesis describes an investigation of melting behavior of three different quartz types, used in the silicon production process, and the effect quartz quality might have on furnace performance. This was done by:

- Measure the softening and melting temperature, and study the melting kinetics, at different holding temperatures in a sessile drop furnace.
- Phase mapping of heat treated quartz, in a rapid heating furnace, with XRD analysis.
- Model the heat distribution in quartz of different sample sizes.
- Implementation of apparent softening and melting temperature to a temperature profile in a silicon production furnace.

From investigations of melting kinetics in a sessile drop furnace, it was observed that quartz has a slow melting rate that increase with increasing holding temperature. It was also observed that melting rate decrease with increasing impurity concentration. Apparent melting temperature were higher than the theoretical of 1713 °C.

Models of heat transfer in quartz indicate that heat conduction is not the rate-limiting factor leading to the slow melting kinetics and high apparent softening and melting temperatures. Since apparent softening and melting temperature were determined by visual inspection of a recorded video of the melting process, the high viscosity of quartz seems to be the main property leading to the high values.

XRD analysis after heat treatment to 1650 °C showed a variation in phase composition between the different quartz types. No correlation between concentration of the different phases and melting kinetics was observed.

The temperature profile with apparent softening and melting temperatures, indicates how the furnace can be divided into the following zones: solid quartz heating zone, softening zone, melting zone and molten quartz zone.

Sammendrag

Denne masteroppgaven beskriver en undersøkelse av smelteegenskaper til tre forskjellige kvartstyper, som brukes i silisiumproduksjon, og effekten kvartskvalitet kan ha på ovnens ytelse. Dette ble gjort ved å:

- Måle myknings- og smeltetemperatur, og studere smeltekinetikk, ved forskjellige holdetemperaturer i en mykningsovn.
- Finne fasesammensetingen i varmebehandlet kvarts ved XRD-analyse.
- Modellere varmefordelingen i kvarts med ulike størrelser.
- Implementere målt myknings- og smeltetemperatur i en temperaturprofil for en silisiumovn.

Fra undersøkelser av smeltekinetikk i mykningsovnen ble det observert at kvarts har en lav smeltehastighet som øker med økende holdetemperatur. Det ble også observert at smeltehastigheten avtok med økende konsentrasjon av urenheter. Målt smeltetemperatur var høyere enn den teoretiske på 1713 °C.

Modellering av varmefordeling i kvarts indikerer at varmeoverføring ikke er den hastighetsbegrensende faktoren som fører til den langsomme smeltekinetikken og de høye myknings- og smeltetemperaturene. Ettersom myknings- og smeltetemperatur ble anslått ved å studere en video av smelteprosessen, kan det virke som at den høye viskositeten til kvarts kan være den viktigste egenskapen som fører til de høye verdiene.

XRD-analysene etter varmebehandling til 1650 °C viste en variasjon i fasesammensetning mellom de ulike kvartstypene. Ingen sammenheng mellom konsentrasjon av de ulike fasene og smeltehastighet ble observert.

Table of Contents

1 Introduction

1.1 Background

Silicon is a semiconducting metalloid. There are three main product groups of silicon. The greatest demand for silicon is in aluminum alloys to strengthen the material. The second major use of silicon is in the production of silicones. It is also widely used as semiconductor and in solar cells. As the use of renewable energy sources are increasing, the demand for silicon grows.

Metallurgical silicon is produced by carbothermic reduction of silica in a submerged arc furnace. The raw materials are silica, SiO_2, in the form of quartz, and various carbon sources such as coke, coal, charcoal and woodchips. The overall reaction for the process is

$$SiO_2 + 2\,C \rightarrow Si + 2\,CO \tag{1.1}$$

Several reaction steps take place in the furnace. Most of the silicon is produced from SiC and SiO after one of the following reactions

$$SiC(s) + SiO(g) = 2\,Si(l) + CO(g) \tag{1.2}$$

$$SiC(s) + SiO_2(s) = Si(l) + CO(g) \tag{1.3}$$
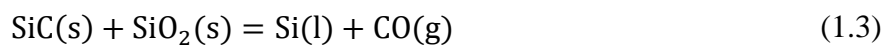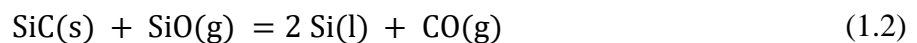
Softening in the upper parts of an industrial silicon furnace can decrease the gas permeability of the charge. If quartz starts to melt too high in the furnace, the amount of SiO_2 will increase in the crater zone and may give unwanted back reaction with silicon to SiO gas. This can affect the furnace operations negatively, and thus decrease the silicon yield. Therefore, it is important to have a good understanding of the high temperature properties of quartz.

1.2 Aim of Work

The aim of this work was to improve the understanding of the impact of the quartz quality to the furnace operation. To achieve a better understanding of the high temperature properties of different quartz types can make it easier to make decisions that will optimize the furnace operations. Melting kinetics, melting mechanism, softening and melting temperature, and phase composition, were studied.

To study the melting kinetics and softening and melting temperature, three quartz types were heated in a sessile drop furnace. A recorded video from the furnace was used to study the melting process. Since phase transitions take place upon heating, it was investigated if this affects the melting behavior. The phase composition was detected with XRD analysis after heat treatment in a rapid heating furnace. To investigate if the heat conduction in quartz is the rate-limiting factor for the melting kinetics, a model of heat conduction was developed in the software COMSOL Multiphysics. Lastly, the results were implemented to a temperature profile of a silicon furnace to evaluate the melting behavior in the furnace.

2 Literature Review

2.1 The Silicon Production Process

Metallurgical silicon is produced by carbothermic reduction of silicon dioxide, SiO_2, also known as silica, in an electric arc furnace. A schematic drawing of a typical silicon production plant is shown in Figure 2.1. The silicate quartz and various carbon sources, such as coke, coal, charcoal or woodchips, are supplied to the top of the furnace and continuously descends. Woodchips are normally added to create a more porous charge mixture and contributes to a more even gas flow by evaporation of moisture during heating. Descending carbon materials are heated and transformed to SiC and reacts with ascending SiO gas producing Si. The SiO gas is produced from quartz, which is assumed to be heated at a rate of approximately 5.5 °C/min. The produced silicon with a purity of approximately 98 % is tapped from the bottom, and gases leave from the top (3).
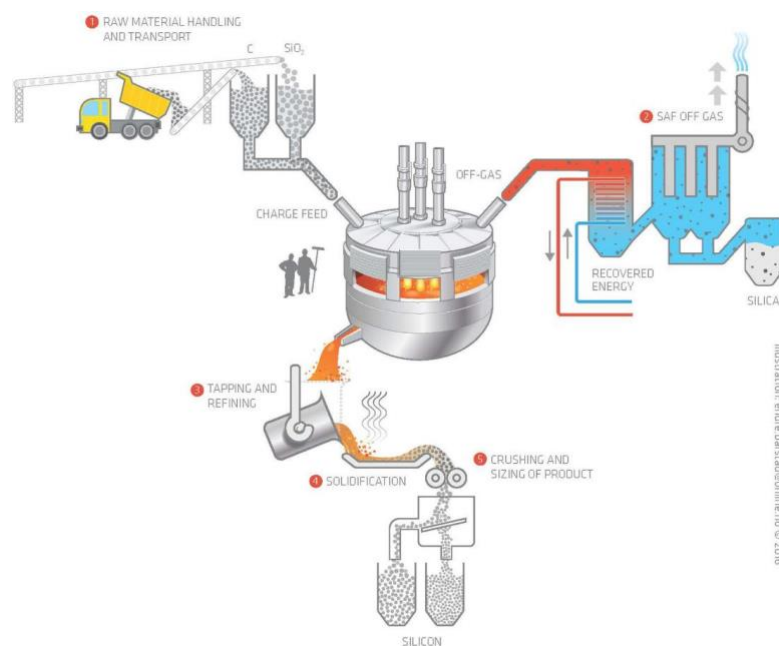

Figure 2.1 *Schematic drawing of a typical silicon production process, reprinted from Kero et Al (4).*

Preferably, the quartz will soften and melt in the high temperature zone in the bottom part of the furnace. If the quartz starts to soften too high in the furnace, charge material can be glued together, and the gas permeability will decrease. This will hinder the ascending gas flow, and thus decrease the silicon yield. Softening high up in the furnace will increase the flow rate of quartz to the lower part of the furnace, as well. The addition of woodchips contributes to decrease the relative amount of quartz and the rate of descending material (5).

The inner structure of the silicon furnace around one of three electrodes is shown in Figure 2.2 (5). A mixture of SiO_2 and SiC will form a bridge of material that prevents material from descending, and a cavity under and on the sides of the electrodes will be formed. Underneath the cavity, there is a pool of liquid silicon and SiC particles. Molten SiO_2 will drip from the cavity wall into the pool and react. If the distance between the charge top and the cavity is small, the area for preliminary reactions is smaller. The recovery reaction for SiO with carbon will be affected as well, due to a higher temperature at the top of the charge. The amount of carbon reactant will also be lower. To break down the cavity, operators have to stoke the charge top regularly (3).
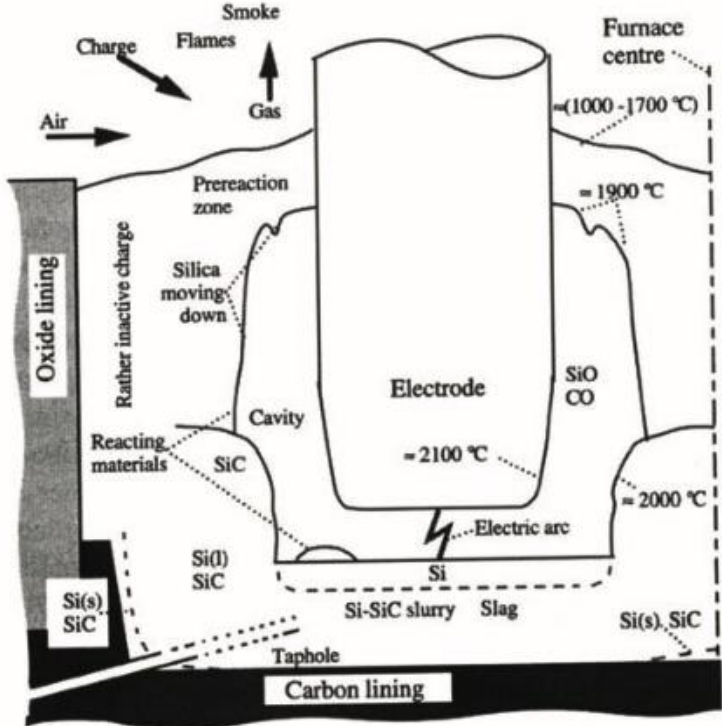

Figure 2.2 The inner structure of a silicon furnace, reprinted from Schei et al. (5).
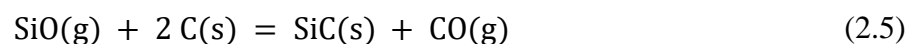
2.1.1 Chemical Reactions in the Silicon Furnace

A series of reactions occurs in different zones in the furnace, but the overall reaction for silicon production is considered to be

$$SiO_2 + 2\,C \rightarrow Si + 2\,CO \tag{2.1}$$

In a system consisting of silicon, carbon and oxygen under the silicon furnace conditions, SiC and SiO are also stable components, making the furnace reactions complex. The top of the furnace, where the raw materials are added, is the low temperature zone, with temperatures between 700 °C and 1300 °C. As the raw materials are descending they will enter the high temperature zone in the crater, where the temperature is well above 2000 °C. An electric arc is generated between the electric tip and carbon containing crater walls. The arc resistance, and a very high electric current, are making the high temperature zone in the crater (6). In this inner main reaction zone, silicon is produced at approximately 2000 °C by reaction (2.2). In addition, SiO is produced in the high temperature zone by reaction (2.3) and (2.4) (6).

$$SiC\,(s) \; + \; SiO(g) \; = \; 2\,Si(l) \; + \; CO(g) \tag{2.2}$$
$$SiO_2(l) + \; Si(l) = \; 2\,SiO \tag{2.3}$$
$$2\,SiO_2 \; + \; SiC(s) = \; 3\,SiO(g) \; + \; CO(g) \tag{2.4}$$

As the SiO gas ascends through the furnace, three different reactions can occur in an outer reaction zone with pre-reactions; it can either react with carbon to produce SiC, as shown in Reaction (2.5), condensate, as shown in Reaction (2.6), or react with CO gas, according to Reaction (2.7), if the partial pressure of CO is sufficient. A schematic presentation of the furnace reactions is given in Figure 2.3.

$$SiO(g) \; + \; 2\,C(s) \; = \; SiC(s) \; + \; CO(g) \tag{2.5}$$
$$2\,SiO(g) \; = \; SiO_2(s.l) \; + \; Si(l) \tag{2.6}$$
$$3\,SiO(g) \; + \; CO(g) \; = \; SiO_2 \; + \; SiC \tag{2.7}$$

According to Reaction (2.8), non-reacted SiO gas reacts to silica in off-gas and reduces the silicon yield. Silica has a very fine particle size and is often considered as a second product from the process. Silica from Elkem has the tradename Microsilica®.

$$2 \, \text{SiO(g)} + \, \text{O}_2(\text{g}) = \, 2 \, \text{SiO}_2(\text{s}) \tag{2.8}$$
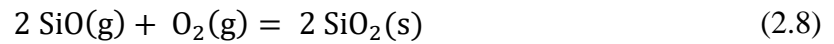
This means that nearly all the quartz must be converted into SiO gas in the high temperature zone to contribute to the silicon yield. To understand the high temperature properties of quartz are therefore important (7).

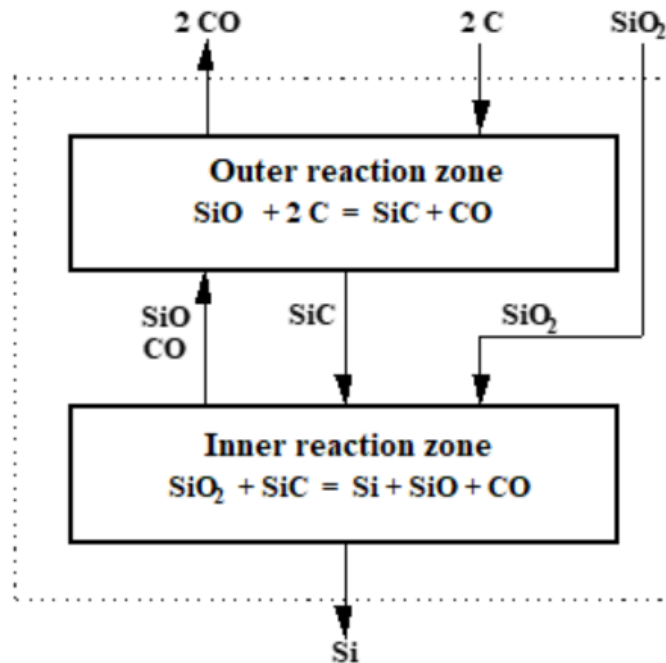**Figure 2.3** *Schematic overview of the furnace when pressure of SiO and CO are equal, as presented by Schei et al (5).*

For Si to be produced after reaction (2.2), the temperature must be above 1811 °C and the partial pressure of SiO above 0.67 atm, as can be seen from Figure 2.4. At lower temperatures SiO gas will react after equation (2.5) and (2.6). This will increase the temperature in the low temperature zone.
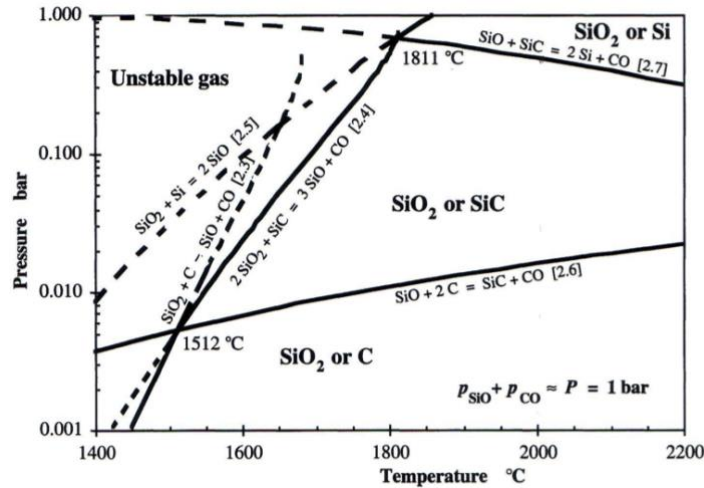
Figure 2.4 *Partial pressure of SiO gas in equilibrium with SiO2, SiC and C as a function of temperature. Total pressure of SiO and CO is 1 atm. The diagram is reprinted from Schei et al. (5).*

2.1.2 Gas permeability in Charge Mixture

High and even gas permeability in the charge mixture is desired. A compact charge will affect the ascending flow of SiO and CO gas negatively, and thus lower the silicon yield. Factors affecting the permeability are the distribution and amount of SiO_2 fines, SiO condensation, and the melting process and volume expansion of quartz during heating (8).

2.1.1.1 Effect of Fines

When the raw materials are added to the furnace, they are shock heated from room temperature to 1000-1300 °C (6). This may lead to disintegration of quartz, and quartz fines with size < 10 mm are produced. (9). Several studies have found large variations in fine generation between different quartz sources upon shock heating (6, 9, 10), see Figure 2.5. If the furnace contains large amounts of fines, the fines will fill the voids between larger particles, increase the charge mixture density, and thus decrease gas permeability. In a study, Edfelt and Nordnes (11) found that important parameters affecting this behavior is the size and distribution of fines in the charge; Smaller fines and layered distribution give a lower permeability. A compact charge will block SiO gas from reacting with carbon to produce SiC. Low gas permeability can also lead to increased gas pressure and velocity followed by formation of gas channels and eruption of materials (11).
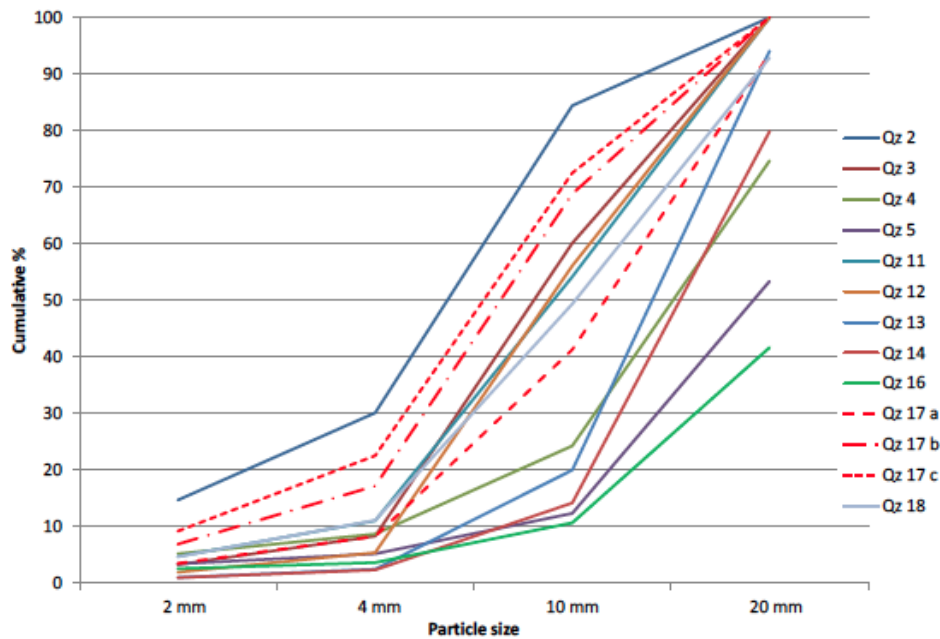
7

Figure 2.5 *Particle size after shock heating to 1500 ℃ for different quartz sources, reprinted from Ringdalen (12).*

2.1.1.2 SiO Condensation

If SiO gas is produced too high in the furnace, in the low temperature zone, reaction (2.3) and (2.4) will cause the partial pressure of SiO to increase and SiO will condensate (8). This will lead to a more compact charge.

2.1.1.3 Heating of Quartz

Softening of quartz is another important parameter affecting the gas permeability. When silica softens, particles can be glued together making a denser charge mixture. Ideally, softening should therefore happen close to the melting temperature. Reaction mechanisms and reaction rates are expected to be affected by the phase change as well (9). During the heating process, quartz will experience several phase transformations (1). The transformation to cristobalite gives a theoretical volume expansion of approximately 17 % at the furnace temperature (7). This gives a more compact charge mixture, and thus lower the gas permeability. Therefore, it is important to know which parameters affecting this behavior to optimize the furnace operations (1).

2.2 Silicon Dioxide Structure

Silicates are materials primarily consisting of silicon and oxygen, the two most abundant elements in the earth´s crust. Rather than characterizing the crystal structures of these materials

in terms of unit cells, it is more convenient to use various arrangements of an SiO_4^{4-} tetrahedron, see Figure 2.6. Various silicate structures result from different ways the SiO_4^{4-} units can be combined into one-, two-, and three-dimensional arrangements (13).
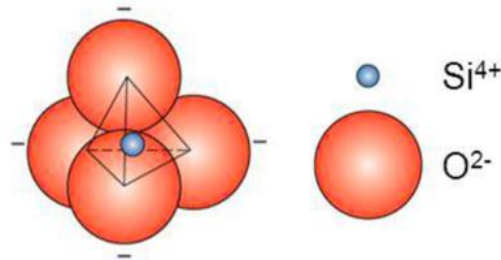

Figure 2.6 *Silicon-oxygen (SiO_4^{4-}) tetrahedron, reprinted from Callister (13).*

2.2.1 Quartz

Chemically, the simplest silicate material is silicon dioxide, SiO_2, known as silica. Structurally, it is a three-dimensional network that is generated when the corner oxygen atoms in each tetrahedron are shared by neighboring tetrahedra. Thus, the material is electrically neutral and all atoms have stable electronic structures. Under these circumstances the ratio of Si to O atoms is 1:2, as indicated by the chemical formula (13).

Quartz is the low temperature polymorph of silica, and thus the one used in silicon production. There are different types of quartz, depending on the level of purity and trace elements. Quartz from different sources has different chemistry. Selection of quartz type and furnace operation can alter the silicon yield, and therefore it is important to have a good understanding of how different parameters are affecting the process. Quartz properties important for the silicon production process are: chemistry, lump size, mechanical strength, thermal strength and softening properties (5, 14).

2.2.2 Silica polymorphism

A crystalline structure of silica is formed when the SiO_4^{4-} tetrahedrons are arrayed in a regular and ordered manner (13). The phase diagram for the silica system, given in Figure 2.7 below, shows that SiO_2 has four main polymorphs which are stable at different temperatures at atmospheric pressure. However, the phase diagram is debated. The polymorphs at atmospheric pressure are α-quartz, β-quartz, HP-tridymite and β-cristobalite (14). Their structures are relatively complicated, and relatively open; that is, the atoms are not closely packed.

Consequently, these crystalline silicates have relatively low densities; for example, at room temperature quartz has a density of only 2.65 g/cm^3. However, the strength of the Si-O interatomic bonds is reflected by a relatively high melting temperature (13). Various melting temperatures have been recorded from different studies. SI Chemical Data reports a theoretical melting temperature of 1713 °C (15).
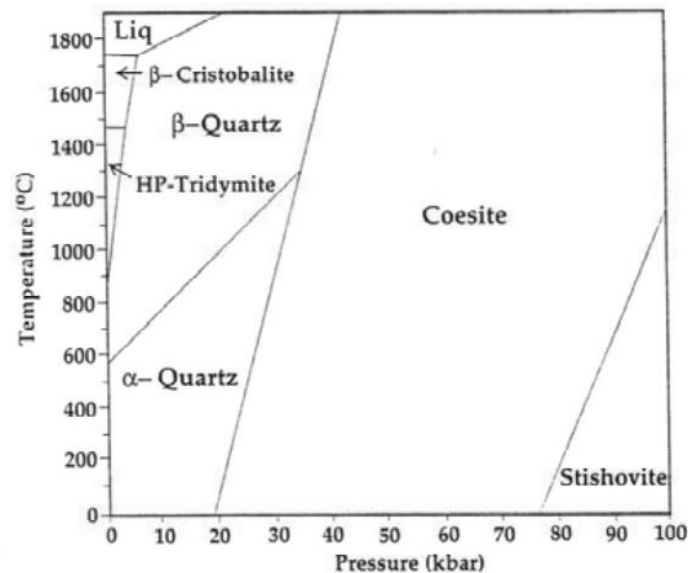

Figure 2.7 Phase diagram of the silica system, reprinted from Aasly (14).

α -quartz is the stable polymorph of silica at room temperature and atmospheric pressure. When quartz is heated in the furnace it will go through several phase transformations before it melts. Some of the transformations are accompanied by a volume expansion as well. The displacive phase transformation from α-quartz to β-quartz takes place from approximately 573 °C, and is reversible upon cooling. α and β denotes low- and high-temperature polymorphs, respectively. The transition has a volume increase of around 0.4 %. The crystal structure changes from trigonal in α-quartz to hexagonal in β-quartz. The α-quartz structure has been interpreted as a distortion of the β-quartz structure (14).

According to the phase diagram, β-quartz is transformed into β-cristobalite at temperatures above 1400 °C, with more rapid transformations at higher temperatures. The transformation is reconstructive and slow, and the amorphous intermediate transition phase is accompanied by a volume expansion of approximately 17 %, depending on temperature (7, 16). In a study, MacKenzie argues that the transformation is sensitive to the ambient atmosphere (17). The transformation leads to fracturing of the quartz, as a result of both the breakage of Si-O bonds and the extensive volume expansion that follows this transformation (14). The structure of
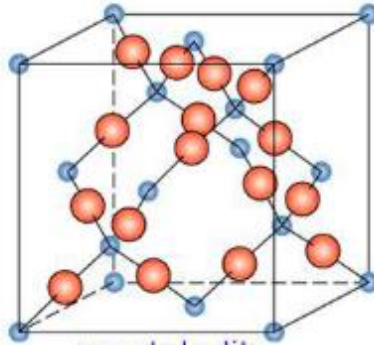
cristobalite is given in Figure 2.8 below.

Figure 2.8 Structure of β-cristobalite, reprinted from Callister (13).

Experiments by Ringdalen (7) indicate that the phase change starts at temperatures below 1400 °C, which is lower than the phase diagram suggests, and the transformation was not complete even after six hours at 1600°C. Kjeldstadli recorded a variation in cristobalite formation between various quartz sources held at 1600°C for different holding times (18). The results are shown in Figure 2.9.
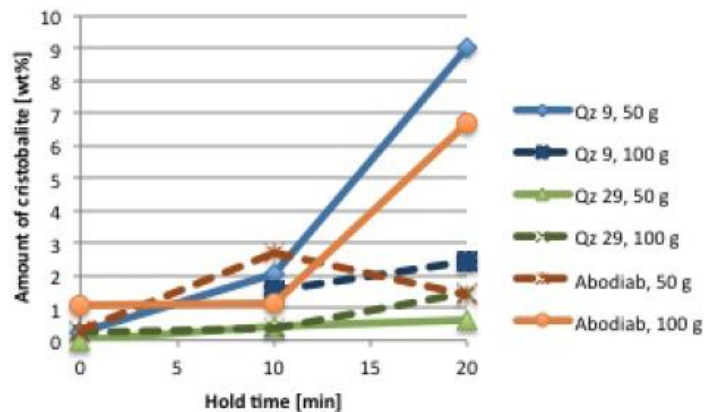

Figure 2.9 Amount of cristobalite in different quartz sources after heating to 1600 ℃ for various holding times, reprinted form Kjeldstadli (18).

HP-tridymite will be formed at approximately 873 °C, according to the phase diagram. A study by Stevens et al. (16) claims that an alkali carbonate mineralizer is necessary for tridymite formation. This means that tridymite is not a stable phase in the pure silica system, and since high purity quartz is used in silicon production there will be little formation of tridymite in the silicon furnaces. (16). However, it is debated whether this transition really takes place, or if β-quartz is transformed directly to cristobalite at a temperature somewhere in between the

temperature for tridymite formation, from the phase diagram, and the melting temperature for silica (7).

Silica can also be made to exist in an amorphous or non-crystalline solid. This form has a high degree of atomic randomness, which is characteristic of a liquid; such a material is called fused silica. As with crystalline silica, the SiO_4^{4-} tetrahedron is the basic unit. Beyond this structure, considerable disorder exists (13). Kjeldstadli measured the amount of amorphous phase after various holding times at 1600 °C as well (18). The amount of amorphous phase was found to be much higher than the amount of cristobalite. This indicates that the rate limiting transition is the reconstructive conversion from quartz to cristobalite (18).
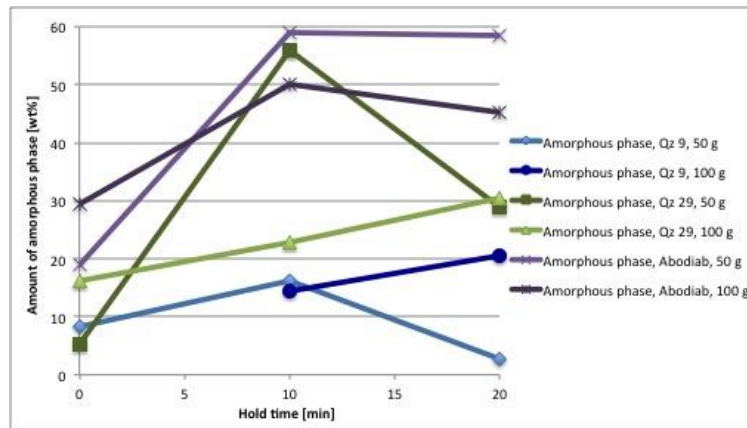

Figure 2.10 *Amount of amorphous silica in different quartz sources after heating to 1600 °C*
for various holding times, reprinted form Kjeldstadli (18)

2.2.2.1 Mechanism for Phase Transitions

The mechanism for phase transitions, and where in the sample it starts, is not fully understood. Wiik (19) argues that the phase transformation from quartz to cristobalite is homogeneous. If this is the case, the phase transformation to cristobalite starts at nucleation sites evenly spread throughout the sample. Since quartz has a higher density than the transition phase between quartz and cristobalite, the volume will expand. This causes tension in the sample, leading to cracks in the parts still being quartz. The reconstructive transformation, involving the breaking of Si-O bonds, will result in an extensive fragmentation of the transition phase. According to Wiik, some studies have found that partially converted quartz samples were easily crumbled under pressure from the fingers. This supports the theory that the transition phase is fragmented, and the phase transformation is homogeneous.

Images of quartz taken with electron probe micro analyzer (EPMA) in a study by Nordnes (20), showed cristobalite formation spread throughout the samples, see Figure 2.11-2.12. This supports Wiik´s theory of a homogeneous phase transformation, from quartz to cristobalite, with nucleation sites distributed over the whole sample.

Figure 2.11 Quartz sample before heat treatment.
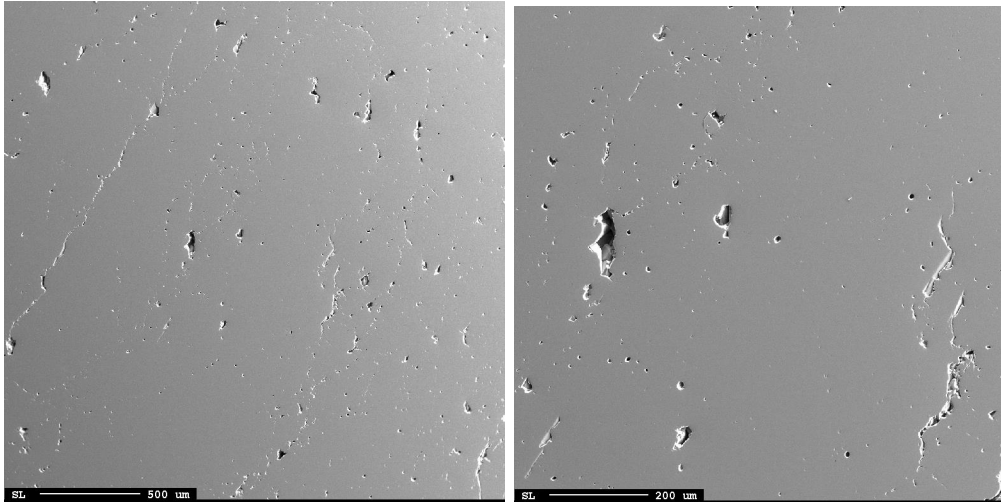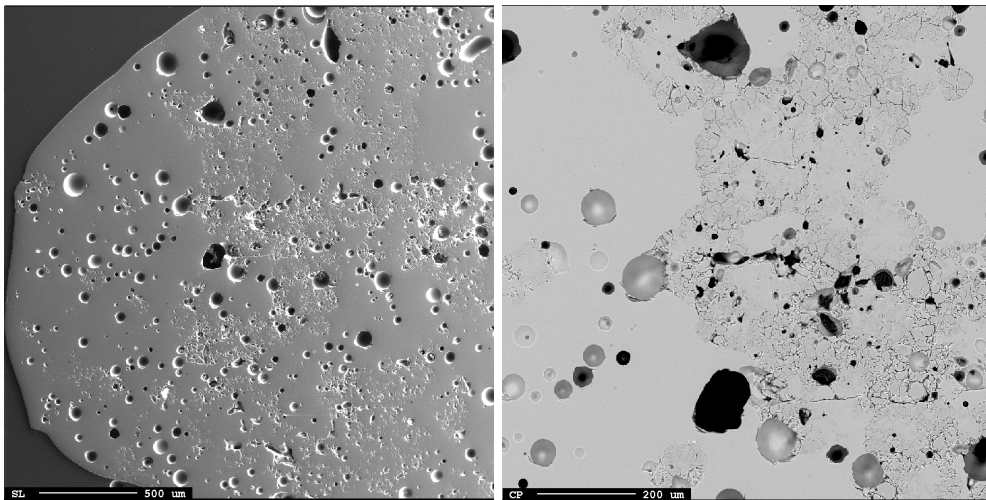

Figure 2.12 Quartz after heat treatment to 1750 °C. High porosity and cristobalite spread throughout the whole sample can be observed.

2.2.3 Volume Expansion

Most solid materials expand upon heating and contract when cooled. Heating or cooling affects all the dimensions of a body, with a resultant change in volume. Volume changes with temperature may be computed from

$$\frac{\Delta V}{V_0} = \alpha_v \Delta T \qquad (2.9)$$

where ΔV and V_0 are the volume change and the original volume, respectively, ΔT is the temperature change, and α_v symbolizes the volume coefficient of thermal expansion. In many materials, the value of α_v is anisotropic; that is, it depends on the crystallographic direction along which it is measured (13). The thermal expansion for quartz itself is small, but varies extensively during the phase changes. The expansion varies for the different crystallographic directions, hence it is an anisotropic material (21).

As mentioned, the theoretical volume expansion for the transition from quartz to cristobalite is approximately 17 % at furnace temperature. Figure 2.13 shows the temperature dependence of the specific volume for quartz, cristobalite and tridymite.

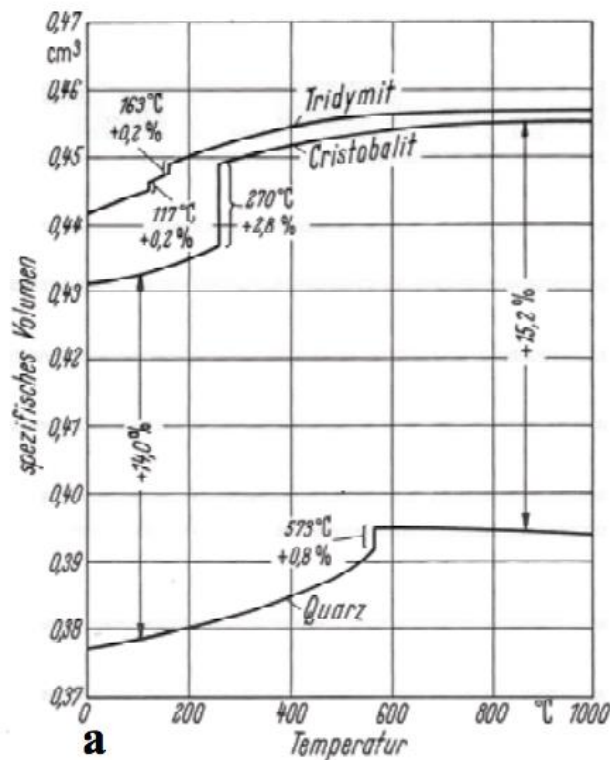**Figure 2.13** *The temperature dependence of the specific volume for quartz, cristobalite and tridymite, as presented by Salmang and Scholze (22).*

Earlier investigations on heating of quartz in a sessile drop furnace, shows a steep increase in volume expansion after around 1500 °C and a decrease after around 1700 °C (7, 23). Besides this, the studies have failed to show any correlation between temperature and volume

expansion. Some experiments even showed a larger volume increase than the theoretical expansion for the phase change, and the expansion showed large variations between samples. However, differences between different quartz sources were observed. Temperature dependence on volume expansion of different quartz types from a study by Ringdalen et al. (7) and Ringdalen and Tangstad (1) is presented in Figure 2.14.
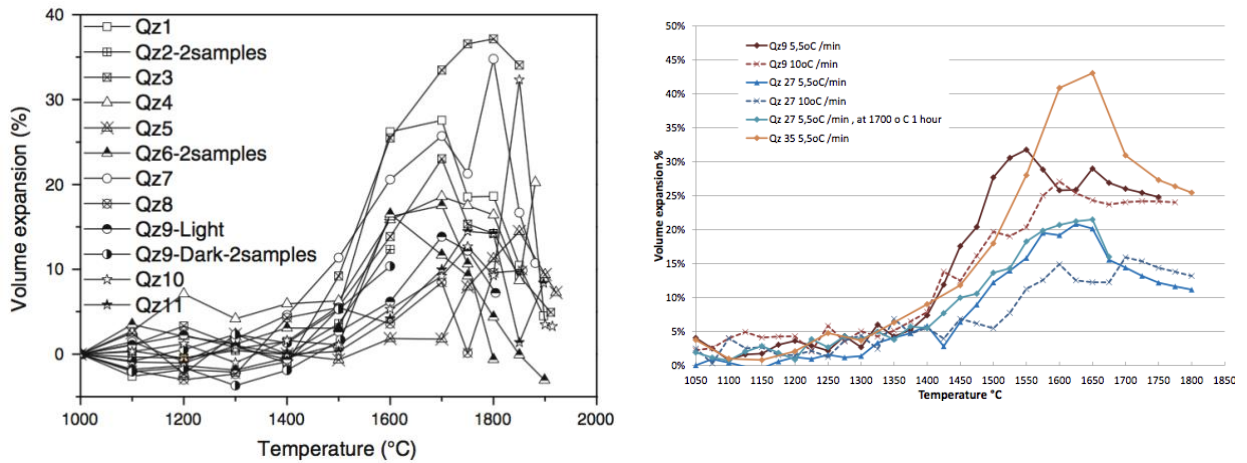

Figure 2.14 *Temperature dependence on volume expansion of quartz samples of different types, reprinted from Ringdalen et al. (left) (7) and Ringdalen and Tangstad (right) (1).*

2.3 Softening and Melting Properties of Silica

The melting temperature of a substance is the temperature at which it changes state from solid to liquid. As energy flows into the solid, the random vibrations of the atoms increase as the temperature rises. Eventually, the atoms become so energetic that they break loose from their lattice positions, and the change from solid to liquid occurs. At the melting temperature, equilibrium between the solid and liquid phase is established (24).

Which phase a substance is in, and which phase transitions that take, depends on temperature and pressure. In order for equilibrium to be established between two phases, the chemical potential, μ, must be the same for both phases. For a pure substance, chemical potential must be equal to the molar Gibb's energy, G_m:

$$\mu = \left(\frac{\partial G}{\partial n}\right)_{T,P} = G_m \tag{2.10}$$

15

This means that Gibb's energy for a pure substance must be the same for the two phases, in order for these to be in equilibrium (25).

The curves in the silica phase diagram given in Figure 2.7 represent equilibrium conditions between the two phases they separate. This means that the melting temperature of silica is represented by the curve between β-cristobalite and liquid, between 1700 °C and 1800 °C. Along this line equilibrium between solid and liquid is established, and silica will melt or solidify. If the temperature is increased above this line, β-cristobalite will melt.

As mentioned, the softening properties are another thermomechanical property important for the furnace performance, as it affects the permeability and reaction rates in the furnace. The softening temperature is defined as the temperature at which the quartz starts to melt and lose its sharp edges. Ideally, the quartz descends to the cavity walls before it starts to melt, and droplets of molten quartz starts to drip from the cavity wall into the pool, where the Si forming reaction takes place. Therefore, it is desired for the softening temperature to be as close to the melting temperature as possible (26). According to Kallfelz (27), charge material glued together, due to softening and melting in the upper parts of the furnace, will become electrically conductive and alter the electric paths in the furnace, and even reduce the power of the arc.

2.3.1 Experimentally Measured Softening and Melting Temperature

In several studies, melting temperatures above the theoretical of 1713 °C have been measured. This includes melting experiments in a sessile drop furnace performed by Nordnes (20). In this study, it was also found that apparent melting temperature and melting kinetics decrease with decreasing holding temperature, see Figure 2.15 below.
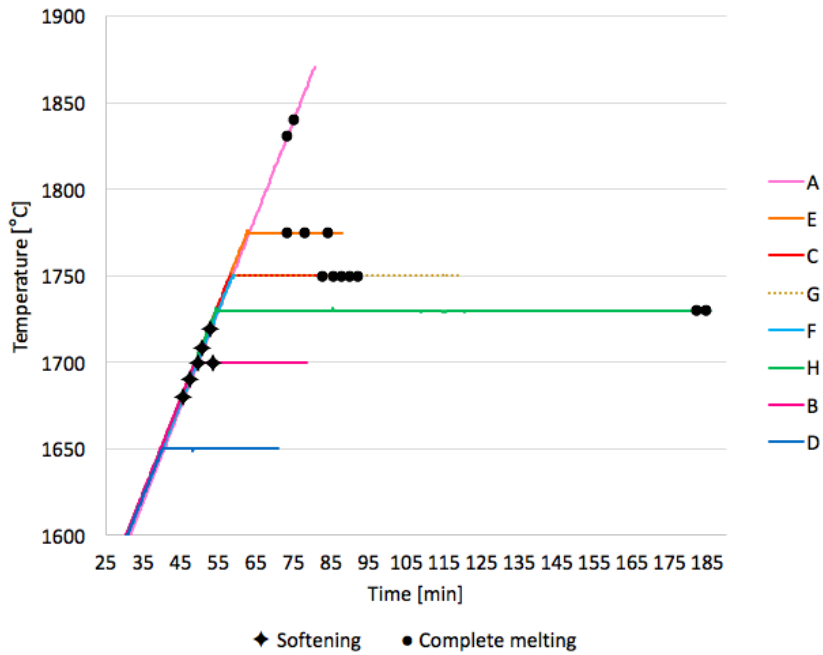
Figure 2.15 *Apparent softening and melting temperature for quartz samples under different temperature conditions.*

From investigations by Ringdalen et al. in a sessile drop furnace (1), melting temperatures in the range 1790 °C to 1900 °C were recorded. It was also observed that apparent temperatures for softening and melting varied considerably between various quartz sources, and that a higher heating rate lead to a higher softening and melting temperature, see Figure 2.16.
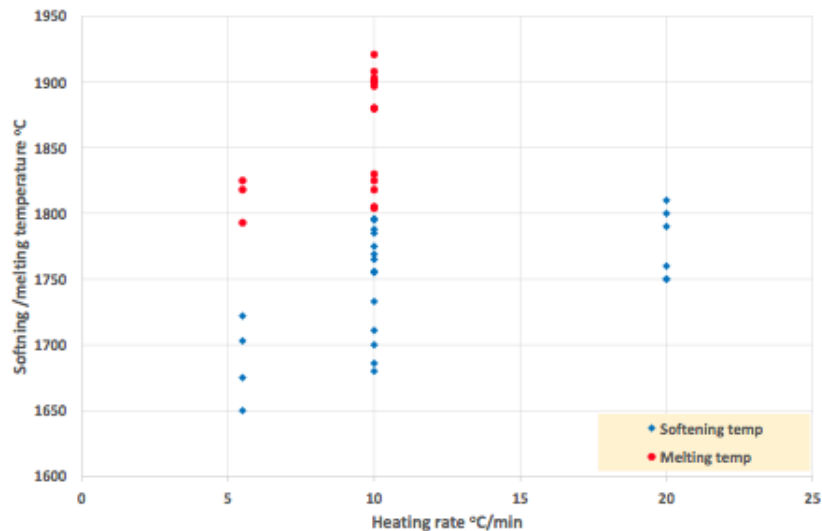

Figure 2.16 *Apparent softening and melting temperature for quartz under different heating rates, reprinted from Ringdalen et al.* (1).

17

2.3.2 Effect of Impurities

Equilibrium between the different phases in a phase diagram is a function of the variables of the system. This means that trace elements in the quartz can alter the melting temperature. The impurity may be dissolved both in the solid and liquid phases (28). According to the Alkemade theorem melting temperature will be lowered when impurities are present (29). Different quartz types contain different trace elements of varying concentration. For systems with several compounds the effect can be complex (28).

As mentioned, the industry has requirements when it comes to quartz properties, such as impurity elements. Both volume expansion and melting properties vary considerably between quartz sources (1). For industrial quartz, trace elements such as Al_2O_3, Fe_2O_3, CaO, Na_2O, K_2O and P_2O_5 are common with concentrations up to 0,5 % (30). Generally, elements more noble than Si tend to end up in the product, whereas the volatile elements follow the off-gas (5). However, the furnace reactions are more complex, and the distribution of impurities in the raw materials will affect where the elements go. It has also been observed that some elements, especially alkalis, may lower the melting temperature (26).

Quartz, cristobalite and amorphous silica have been found to coexist in heat treated quartz kept for a relatively long time at temperatures between 1500 °C and 1700 °C (7, 18, 31). This indicates that the phase transformation from quartz to cristobalite is relatively slow, and that solid and liquid coexist in a melting interval from a temperature lower than the theoretical melting temperature. A variation of the relative amount of the phases between different quartz sources has been observed as well. This means that the constituents will change the rate of the solid-state phase transformation as well as the melting temperature (7).

Investigations by Ringdalen and Tangstad (1) showed large variations in melting behavior for different quartz sources. The experiments showed a decrease in apparent softening temperature as a function of FeO content, when the sample with the highest concentration was omitted, see Figure 2.17. No correlation between content of Al_2O_3 or alkalis and measured softening temperature was observed.
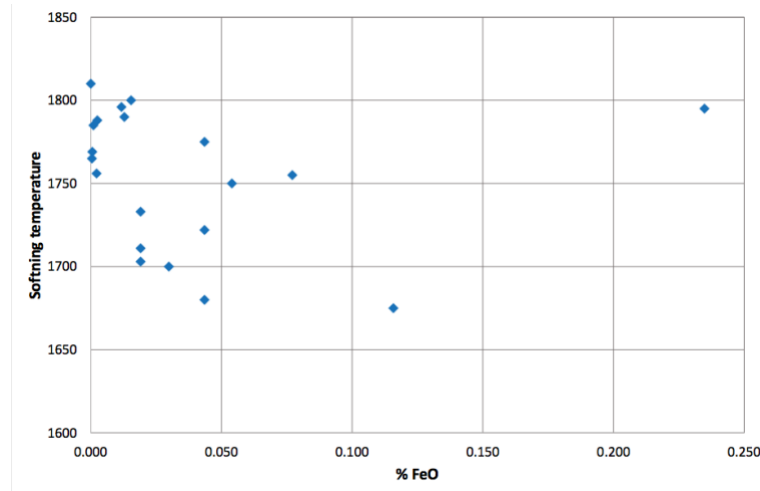
18

Figure 2.17 *Apparent softening temperature of quartz as a function of FeO content, as represented by Ringdalen and Tangstad (1).*

Previous studies by Jusnes et al. (9), Ringdalen (12) and Paulsen and Bakken (10), indicate that impurities in quartz not only affect the melting behavior, but also the level of disintegration. Jusnes et al. (9) used shock heating in their experiments, and the results showed larger variations between the different quartz types than between the parallels of each sample. When quartz disintegrates, the total surface area will increase. This will lead to a higher reaction area in the upper parts of the furnace and lower the charge permeability. For Si to be produced, the temperature must be above 1811 °C, as shown in Figure 2.4. Therefore, it is favorable that the quartz does not start to react in the upper parts of the furnace. In zones with temperatures lower than 1811 °C SiO gas might be produced, and thus lower the silicon yield since the SiO gas will leave the furnace before it is reduced to Si. The energy distribution in the furnace might be affected if the rate of the reactions in the upper parts of the furnace increase (9).

2.3.3 Mechanism of Melting

As for the mechanism of phase transformations, the mechanism of melting is not fully understood, and researchers have come to different conclusions. A melting process might be described by classical nucleation theory. Nucleation is the initial process in phenomena such as vapor condensation, crystal nucleation, melting and boiling, and is defined as the localized emergence of a distinct thermodynamic phase at the nanoscale that macroscopically grows in size with the attachment of growth units. These phase changes are the result of atomistic events driven by thermal fluctuations (32).

19

Homogeneous nucleation is a significantly studied process that occurs when a system initially in a state of stable thermal equilibrium becomes metastable as a result of thermal fluctuations, and there is no role for foreign surfaces (32). This is the mechanism Wiik (19) and Nordnes (20) suggested for the phase transformation from quartz to cristobalite in their studies.

A study by Ainslie et al. (33) claims that all experiments so far indicate that the melting process of silica is heterogeneous. This means that nucleation starts at the surface of a crystal, forming a liquid film that propagates inwards. They also found that this will happen at slight superheating.

2.4 Melting Kinetics

2.4.1 Rate Equations

The temperature dependence of thermally activated processes is commonly explained in terms of rate laws, such as the Arrhenius equation

$$k_A(T) = A \exp\left(-\frac{E}{RT}\right)$$

(2.11)

where $k_A(T)$ is the "apparent rate constant" at temperature T, A is the area, R is the gas constant (Jmol^{-1}K^{-1}), T is the absolute temperature (K), and E is referred to as the apparent activation energy for the reaction (Jmol^{-1}). These thermally activated processes include both chemical and diffusional processes (34).

The Arrhenius equation can be put in its most useful form by finding the specific reaction rate at a temperature T_0, and at a temperature T, and taking the ratio to obtain

$$k(T) = k(T_0) \exp\left(\frac{E}{R}\left(\frac{1}{T_0} - \frac{1}{T}\right)\right)$$

(2.12)

This equation says that if we know the specific reaction rate $k(T_0)$ at a temperature, T_0, and we know the activation energy, E, we can find the specific reaction rate $k(T)$ at any other temperature, T, for that reaction (35).

Not much literature on melting kinetics exists. However, some information can be drawn from the Arrhenius equation. Nordnes (20) suggested that the rate of a melting process of quartz might be written as

$$\frac{dr}{dt_{melt}} = kf(A)f(T)f(driving\ force) \tag{2.13}$$

when some assumptions are made, where dr/dt_{melt} is the melting rate, k is the rate constant, $f(A)$ is a function of area, $f(T)$ is a function of temperature, and $f(driving\ force)$ is a function of the driving force for the process. In the deviation, it is assumed that heat transfer is not the rate limiting property for the melting process. The driving force for the melting process is the temperature difference between theoretical melting temperature and experimentally recorded melting temperature (35). Viscosity, and the change in viscosity upon heating, will alter the melting temperature (33). Since only one compound was used in the experiments, the effect of viscosity is given by the temperature function.

2.4.2 Experimentally Measured Melting Rate

From the study by Ainslie et al. (33) mentioned earlier, claiming that the melting process of silica is heterogeneous, it was possible to determine the melting rate by measuring the layer of melted glass phase formed at a quartz substrate. The quartz sample and kinetics plots are given in Figure 2.18. It can be observed that a higher furnace temperature leads a higher melting rate.
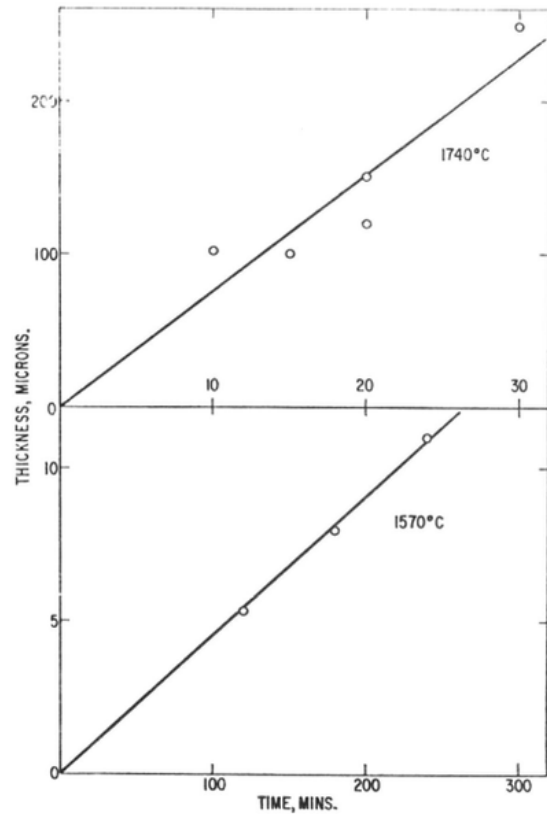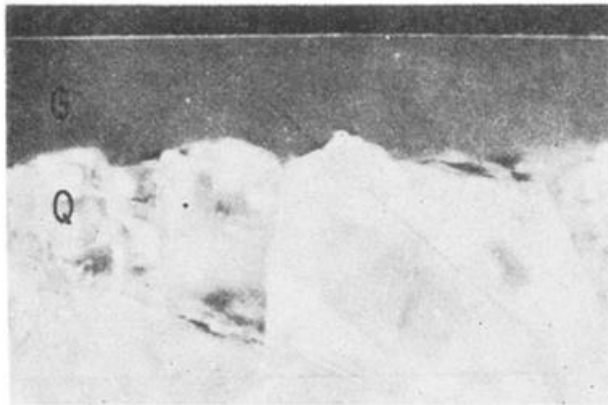
Figure 2.18 *Glass phase (G) formed on quartz (Q) under heating of quartz at 1730 ℃ for 15 minutes (left) and thickness of melted layer as a function of time at 1740 ℃ and 1570 ℃ (right), reprinted from Ainslie et al. (33).*

A study by Nordnes (20) indicates that melting rate of quartz increase with increasing furnace temperature. This agrees with the observations by Ainslie et al. (33). A constant heating rate of 5,5 °C/min to complete melting, well above 1800 °C, gave the highest melting rate. For experiments with holding times at lower temperatures, the overall trend was that the melting rate at holding temperature increased with increasing temperature at holding time, as can be seen from Figure 2.19.
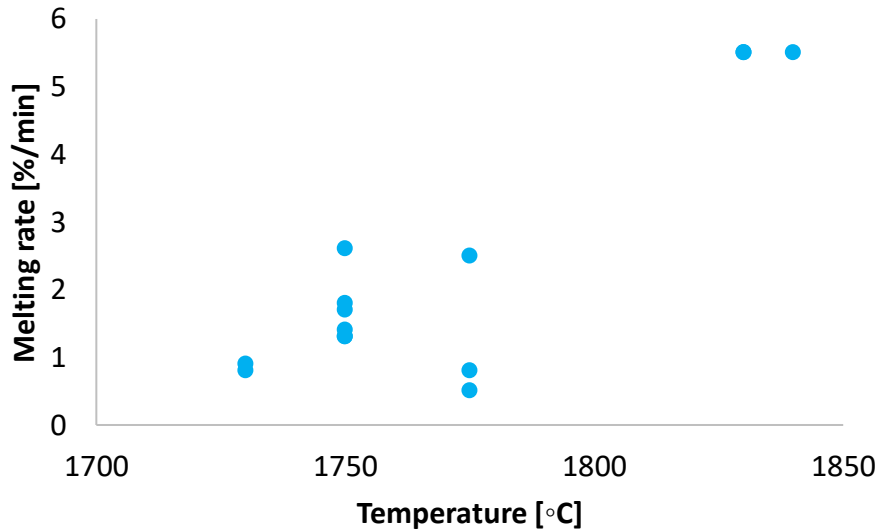
Figure 2.19 *Melting rate at different holding temperatures (1730 °C, 1750 °C and 1775 °C) and at a heating rate of 5,5 °C /min (1830 °C and 1840 °C), reprinted from Nordnes (20).*

2.4.3 Viscosity

Zumdahl defines viscosity as the resistance of a liquid to flow (24). Thus, the viscosity corresponds to the thickness. It decreases with increasing temperature and becomes more liquid-like (1). Temperature effect on viscosity for silica is given in Figure 2.20 below.

Ainslie et al. (33) found that the viscosity of a melt will affect its melting kinetics. At the melting temperature, liquid silica has a high viscosity around 2×10^7 Poise, and will therefore behave nearly as a solid (1). For a melt with low viscosity, the heat absorptions will be so fast that the interior of a crystal will melt before it becomes superheated. For melts with high viscosity, such as quartz, the heat absorptions will be slower, and high superheating can be obtained (33). The high viscosity will slow down the heat transfer and give high superheating (33). A study by MacKenzie (17) found that quartz can sustain superheating of 300 °C a considerable period of time. Investigations by Hack et al. (2) suggest that viscosity can be altered by contaminants, as shown in Figure 2.21.
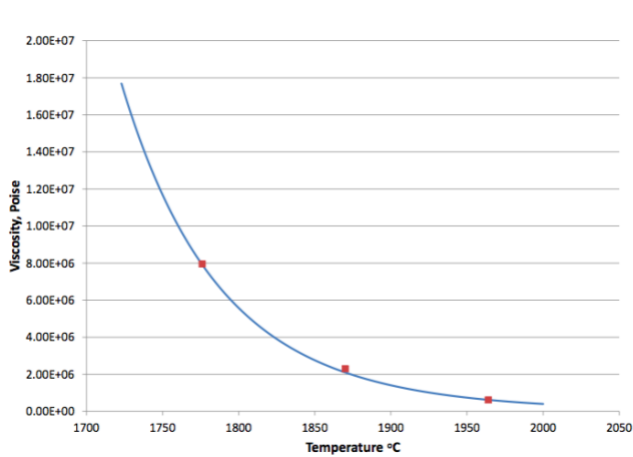
23

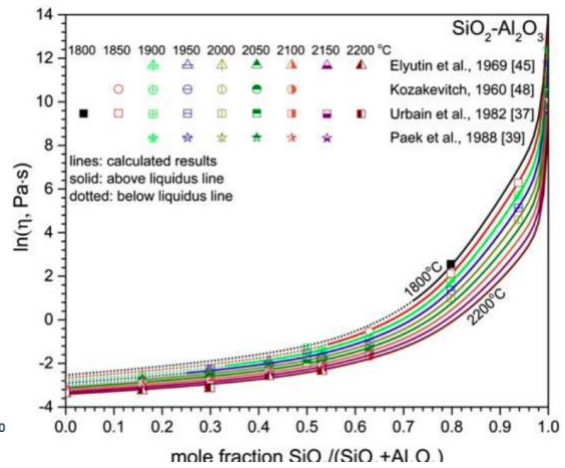**Figure 2.20** *Viscosity of molten silica, reprinted from Ringdalen et.al. (1).*

Figure 2.21 *Viscosities in SiO₂-Al₂O₃ melts, reprinted from Hack et.al. (2).*

2.5 Heat Conduction

Heat exchange between objects of different temperatures, may be done by three different mechanisms: convection, radiation or conduction. Thermal conduction is the spontaneous transfer of thermal energy due to a temperature difference. It is a material property that indicates a materials ability to conduct heat. Thermal conduction always takes place from a region of higher temperature to a region of lower temperature, and acts to equalize temperature differences (36). In metallic solids, energy is transferred by "free" electrons. In solid silica, conduction is the main mechanism of heat transfer. Transfer of heat by conduction follows Fourier´s law for heat conduction in fluids or solids:

$$\frac{q_x}{A} = -\lambda \frac{dT}{dx} \tag{2.14}$$

where q_x is the heat-transfer rate in the x direction, A is the cross-sectional area normal to the direction of flow of heat, T is temperature, x is distance, and λ is the thermal conductivity. The quantity q_x/A is called the heat flux in, and the quantity dT/dx is the temperature gradient in the x direction. The minus sign in Equation. (2.12) is required because if the heat flow is positive in a given direction, the temperature decreases in this direction (37).

Thermal conductivity of two different types of quartz calculated by Ksiazek (38), and both calculated and experimentally measured values from a study by Car et al. (39), are given in Figure 2.22.
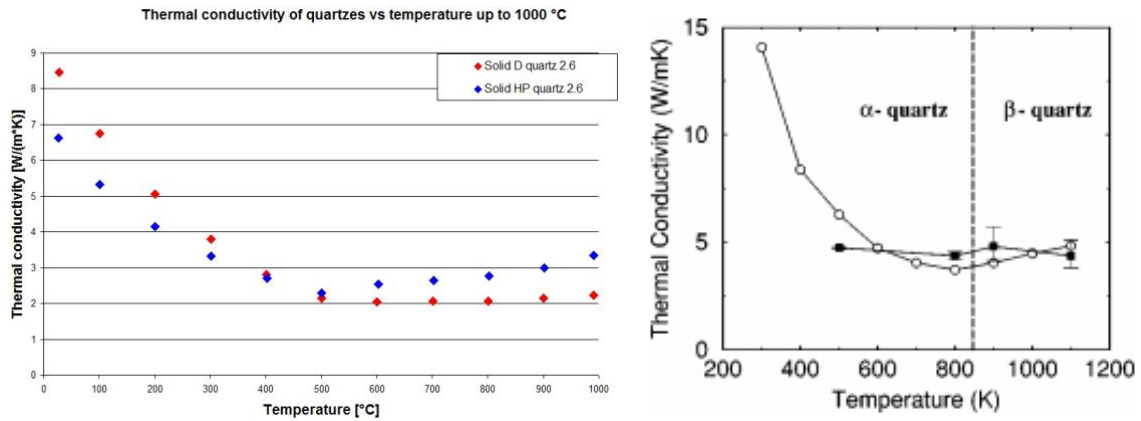
Figure 2.22 *Thermal conductivity of quartzes. D quartz and HP quartz, reprinted from Ksiazek (38) (left), and experimental (circles) and calculated (squares) values, reprinted from Car et al.(39) (right).*

Thermal diffusivity, α, is a property that measures the ability of a material to conduct thermal energy relative to its ability to store thermal energy (38). It is related to thermal conductivity, λ after

$$\alpha = \frac{\lambda}{\rho c_p} \qquad (2.15)$$

where ρ and c_p are the density and specific heat capacity, respectively (37). Both density and specific heat capacity vary considerably with temperature and phase transformations. Values for specific heat from two different sources are given in Figure 2.23 below.
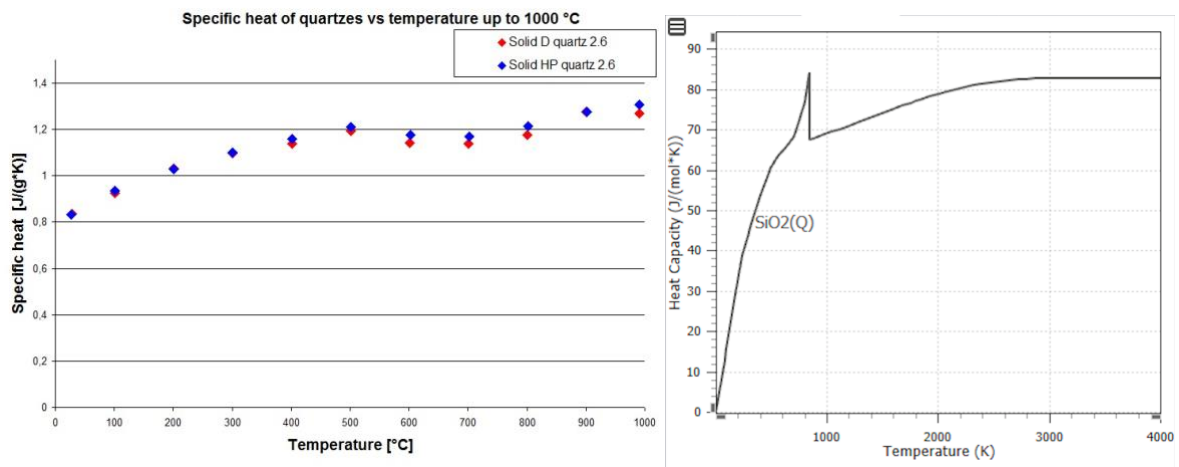

Figure 2.23 *Specific heat of solid quartzes. D quartz and HP quartz, reprinted from Ksiazek (38) (left), and values for pure quartz from the software HCS 9.9 (right).*

25

To study heat conduction inside spherical quartz particles in silicon furnaces, Ksiazek modelled the heat distribution (40). In the models, he used values for density (2600 kg/m^3), specific heat (1300 J/K·kg), and thermal conductivity (2-3 W/m·K) at 1000 °C, taken from a previous work by himself on termophysical properties, see Figure 2.22-2.23 above. Heat distribution in spheres with radius of 5 mm and 5 cm, heated directly up to 1200 °C from room temperature, and held for 60 seconds, is shown in Figure 2.24-2.25 below. The smallest sample seemed to have reached the target temperature, while the largest sample had a temperature difference of 1180 °C between surface and center.
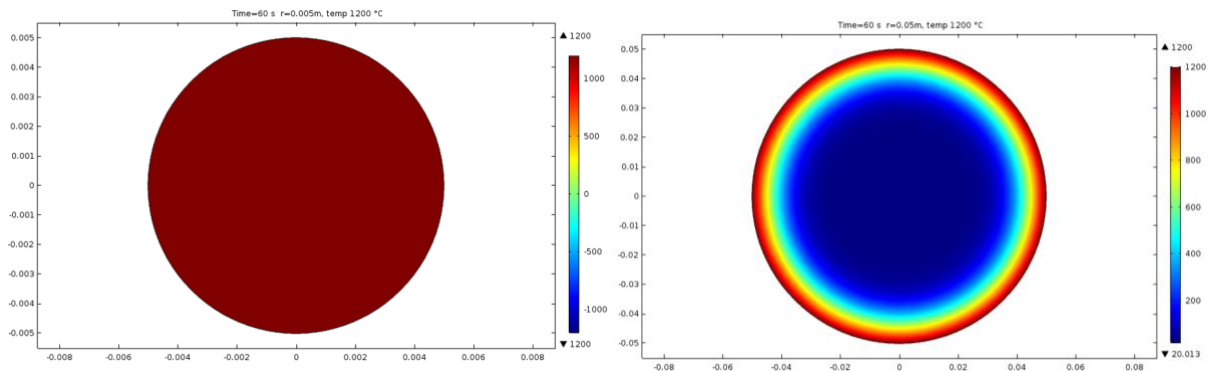

Figure 2.24 *Temperature distribution after 60 seconds in quartz spheres with radius 5 mm (left) and 5 cm (right) heated from room temperature to 1200 °C.*
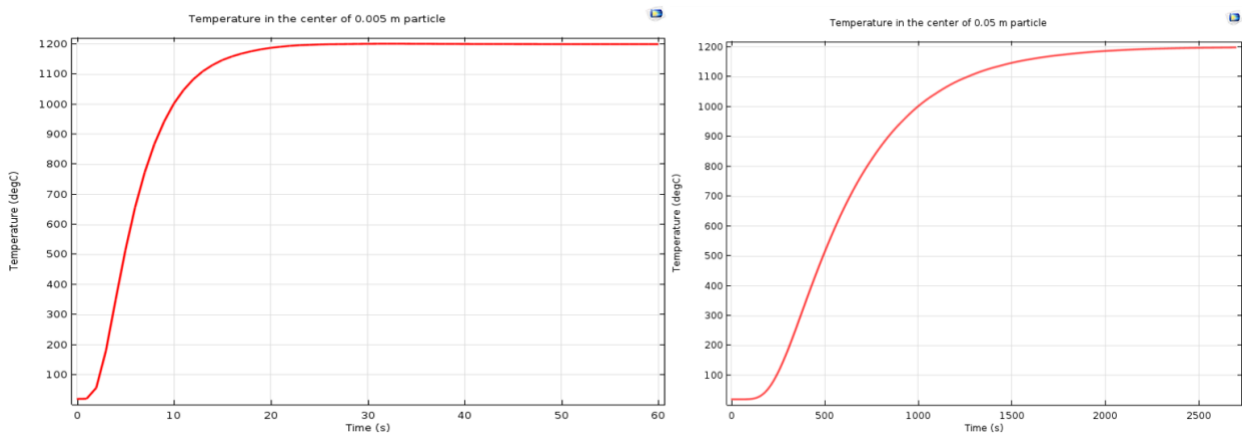
Figure 1.25 *Temperature in quartz spheres with radius 5 mm (left) and 5 cm (right) heated from room temperature to 1200 °C.*

Kjeldstadli (18) modelled the temperature in the center of a quartz sample as a function of time in cooperation with M. Ksiazek. The samples were heated in a furnace at a rate of 57 °C/min. According to the model, it will take around 30 minutes for a sample with a radius of 1 cm to reach 1700 °C, as can be seen from Figure 2.26.

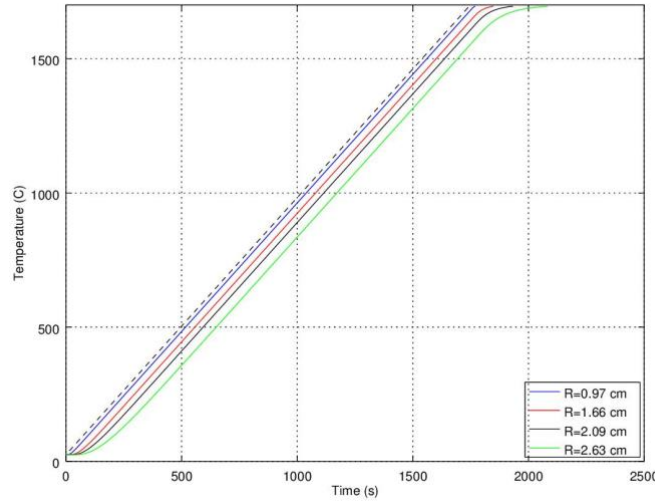***Figure 2.23*** *Time dependence on temperature in the center of spherical quartz samples with different radius, reprinted from Kjeldstadli (18).*

2.6 X-Ray Diffraction

If a substance is non-molecular and crystalline, identification of chemistry and structure is usually carried out by X-ray diffraction (XRD). Each crystalline solid has its own characteristic X-ray powder pattern which may be used as a "fingerprint" for its identification. X-rays used in almost all diffraction experiments are produced in a process that leads to monochromatic X-rays. A beam of electrons, accelerated through a high voltage, strikes a metal target. The incident electrons have sufficient energy to ionize the metal. An electron in an outer orbital immediately drops down and the energy released appears as X-ray. The monochromatic peaks caused by electronic transitions within the atoms have wavelengths characteristic of the structure and elements. This makes it easy to analyze crystalline solids (41).

Amorphous phases, characterized by a high degree of atomic randomness, are more complicated to quantify. To determine the content of amorphous silica in silica samples, a method known as the internal standard method might be used. In this method, the sample is crushed and spiked with an extremely crystalline material of known accurate weight. The weight fraction of the crystalline phases present in the sample is estimated using the equation:

$$W_\alpha = \frac{S_\alpha (ZMV)_\alpha}{\sum_{j=1}^{n} S_j (ZMV)_j} \tag{2.16}$$

27

where S_α is the Rietveld scale factor for phase α, ZM is the mass of the unit cell content, V the volume of the unit cell, and n is the number of phases in the analysis. It relies on the assumption that all phases in the sample are crystalline and have been included in the analysis, and thus equation xxx sums the analyzed concentrations to unity. The presence of the known weight fraction of the crystalline internal standard material could then be used to calculate the corrected weight fraction, $Corr(W_\alpha)$, based on the already calculated weight fraction in the crystalline phases.

$$Corr(W_\alpha) = W_\alpha \frac{STD_{known}}{STD_{measured}} \tag{2.17}$$

where STD_{known} is the weighted concentration of the standard in the sample, and $STD_{measured}$ is the analyzed concentration derived from Equation xxx.

Lastly, the weight fraction of the amorphous phase, $W_{amorphous}$, can be found from

$$W_{amorphous} = 1 - \sum_{j=1}^{n} Corr(W_j) \tag{2.18}$$

3 Experimental

3.1 Softening and Melting Temperature and Melting Kinetics

To measure softening and melting temperature, and study the melting kinetics, of different quartz types, quartz samples were heated in a sessile drop furnace. A recorded video of the melting process in the furnace was used to determine softening and melting temperature.

3.1.1 Experimental Setup

To investigate the melting behavior, a sessile drop furnace was used, see Figure 3.1 for a schematic illustration. The furnace is designed to observe the behavior of a sample on a substrate at high temperature. The sample size is quite small, with a maximum substrate size of 10 mm in diameter and 2 to 5 mm in height. The liquid drop must be small enough to sit on top of the substrate without touching the edges, with a typical sample weight varying from 10 mg to 1 g. The furnace is closed, and contains graphite heat elements, where the substrate and sample are placed. All the heated furnace parts, including the element and heat shields, are constructed of graphite, allowing both extremely fast and slow heating. Desired gas atmosphere, temperature and heating rate can be chosen. The heating process in the furnace is visually recorded by a camera through a silica glass window. A firewire digital video camera with a telecentric lens is used. It is possible to produce images with a resolution up to 1280 x 960 with a ½²CCD sensor. It is possible to measure the wetting angle of the sessile drop and the volume expansion of the sample as well (42).
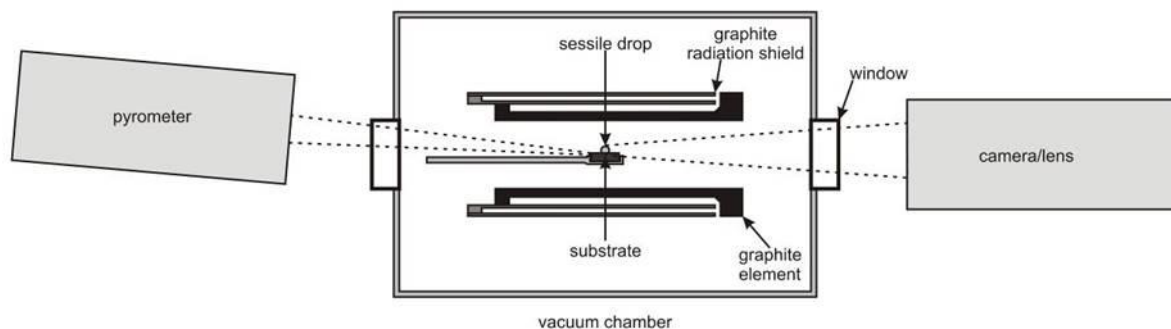
Figure 3.1 *Schematic drawing of a sessile drop furnace, reprinted from Bao et al. (42).*

3.1.2 Materials

Quartz samples of three different types were used in the experiments. The heat treatment was performed with graphite substrates with a diameter of 10 mm and height of 3 mm, made from ISO88 (Tanso). The quartz samples were prepared by drilling cylinders with diameter and height of approximately 4 mm from larger lumps. The materials are shown in Figure 3.2. The bottom and top of the cylinders were polished to make the samples able to stand on the substrate and have an even cylindrical shape.

(a) Samples of the three different quartzes   *(b) Graphite substrate with diameter and*
after heat treatment.   *height of 10 mm and 3 mm, respectively.*

Figure 3.2 *Samples and substrate used in the sessile drop experiments.*

Table 3.1 *Concentration of trace elements in two of the quartz types used in this work (B and C), and one used in a previous work by the author (D), supplied by Elkem (30). The samples are analyzed with XRF.*

Quartz type	%Al$_2$O$_3$	%Fe$_2$O$_3$	%CaO	%Na$_2$O	%K$_2$O	%total impurities
B	0,492	0,3493	0,0046	0,0037	0,0754	0,925
C	0,015	0,0035	0,0044	0,0028	0,0016	0,0273
D	0,026	0,0068	0,24	0,0073	0,0129	0,293

3.1.3 Method

A total of 27 experiments were executed in the sessile drop furnace; four different heating programs for each quartz type with one to three parallels. The quartz samples were placed on the graphite substrates and heated under Ar atmosphere with a flow rate of 0,5 L/min. The heating rate was 300 °C/min from room temperature until 900 °C, 67 °C/min from 900 °C to 1500 °C, and 5,5 °C/min from 1500 °C until end of test or temperature at holding time. All experiments were stopped at complete melting. Heating rates for all tests are given in the plot in Figure 3.3 below. Conditions for all experiments are listed in Table 3.2.
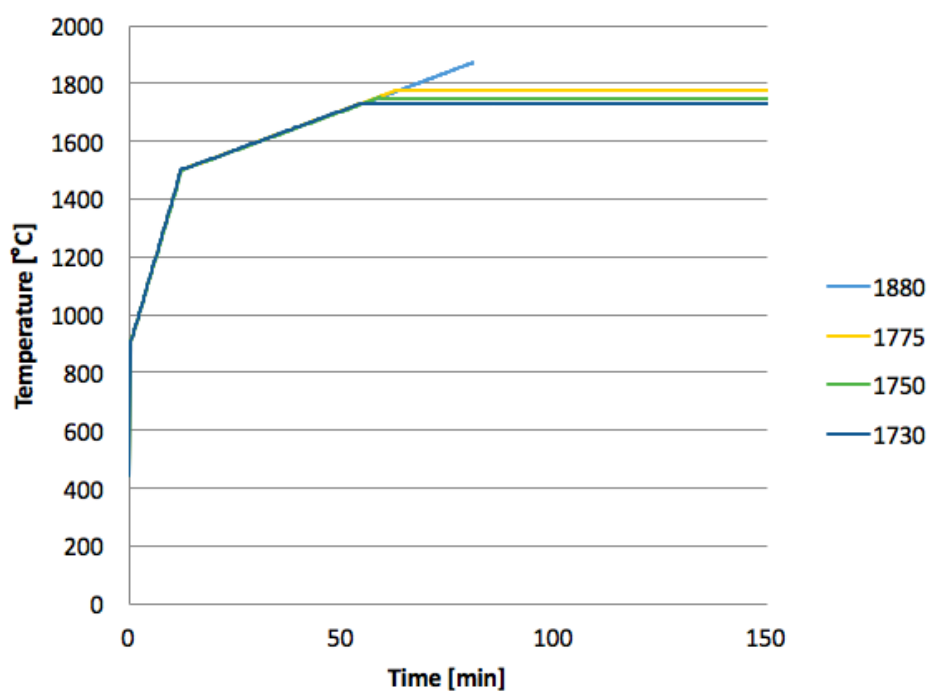

*Figure 3.3* *Heating rates used in the sessile drop furnace.*

Table 3.2 *Conditions for the heat treatments. One to three parallels were executed of each*
test.

Test	Numbers of parallels	Quartz type	Highest temperature of test [°C]	Heating rate after 1500 °C [°C/min]	Atmosphere
A	3	A	1830-1850	5,5	Ar
B	3	A	1775	5,5	Ar
C	3	A	1750	5,5	Ar
D	1	A	1730	5,5	Ar
E	3	B	1880-1830	5,5	Ar
F	2	B	1775	5,5	Ar
G	2	B	1750	5,5	Ar
H	1	B	1730	5,5	Ar
I	3	C	1820-1830	5,5	Ar
J	3	C	1775	5,5	Ar
K	2	C	1750	5,5	Ar
L	1	C	1730	5,5	Ar

A recorded video of the heating process was analysed afterwards to determine the:

- Softening temperature: When the shape of the particle has lost its sharp edges.
- Temperature at complete melting: When the droplet is round, with no artefacts.

Figure 3.4 below shows a quartz sample heated from room temperature to complete melting at 1830 °C, at the beginning of the test (a), at the beginning of melting (b) and at complete melting (c).
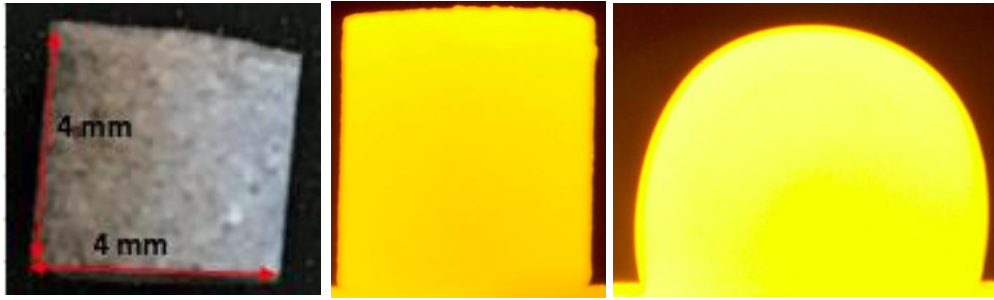
| *(a) Sample before heating.* | *(b) Sample at softening temperature.* | *(c) Completely melted sample at 1830 °C.* |

Figure 3.4 *A quartz sample heated from room temperature to 1830 °C in a sessile drop furnace.*

3.2 Phase Mapping of Heat Treated Quartz

To investigate the dependence of phase composition on melting behavior for the various quartz types, quartz samples were heated to 1650 °C in a rapid heating furnace without holding time and analyzed with XRD. The content of amorphous silica is the most important phase measured from these experiments.

3.2.1 Experimental Setup

The heat treatment was done in a rapid heating furnace, a Nabertherm LHT04, as shown in Figure 3.5. The heating chamber of the furnace had a height of 15.2 cm and width of 15.0 cm. Heating elements are placed on the left and right walls. The furnace only uses air atmosphere, and temperature programs can be chosen manually. Samples was placed on substrates on the furnace floor.
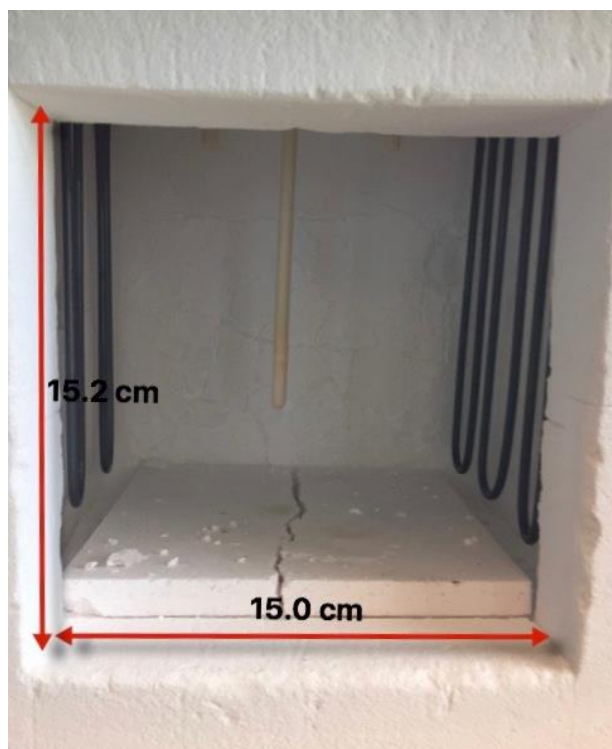
Figure 3.5 *Interior of the rapid heating furnace used in the experiments, a Nabertherm*
LHT04, reprinted from Kjelstadli (18).

3.2.2 Materials

Quartz of the same three types as used in the sessile drop experiments were used. The samples were prepared by using a hammer on larger lumps to get pieces with masses of 15±5 g. It was difficult to make the shape and weight of the samples equal, and thus the diameter will vary. Three samples of each quartz type were made, all from different lumps, giving a total of nine samples. Samples of two of the quartzes are shown in figure 3.6. To avoid any contamination in the furnace, the samples were placed on alumina substrates, see Figure 3.7.

Figure 3.6 *Samples of two of the quartz types used in the rapid heating experiments. Mass of the samples is 15±5 g.*

Figure 3.7 *Alumina substrate, with diameter of 5 cm and height of 0,5 cm, used in the rapid heating experiments.*

3.2.3 Method

The three parallels of one quartz type were heated at a time. The samples were placed on alumina substrates in the center of the furnace floor. A heating rate of 50 °C/min was used from room temperature until 1500 °C, and a heating rate of 5,5 °C/min was used from 1500 °C until 1650 °C, where the samples immediately were taken out and cooled at sand in room temperature. Before the furnace was heated, the door was closed to isolate the furnace. The experiments were done in air atmosphere. The heating rate is shown in the plot in Figure 3.8.
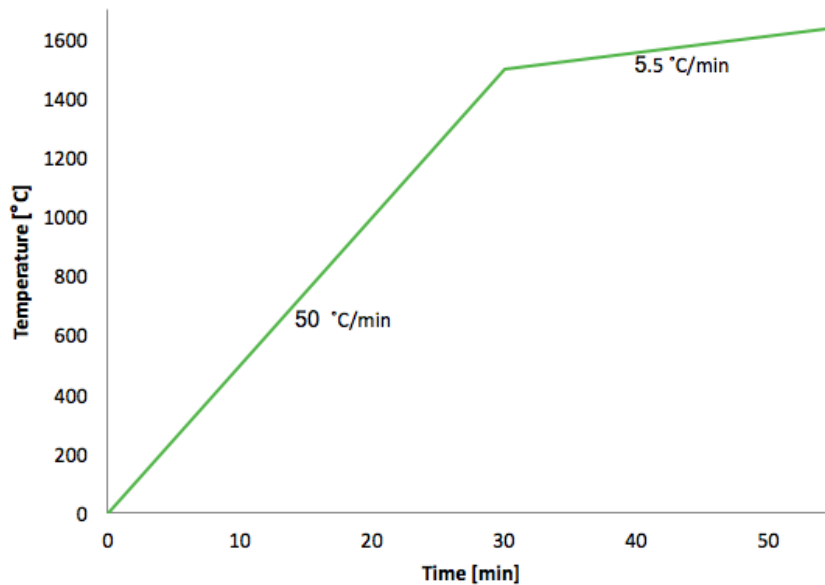
Figure 3.8 *Heating program used in the rapid heating furnace.*

3.2.4 X-ray Diffraction

The aim of the XRD analysis was to measure the amount of amorphous phase, to see if there was a variation between the different quartz types corresponding to the measured melting rates from the sessile drop experiments. The analysis was performed by Julian Tolchard (SINTEF) after the internal standard method and the procedure presented by Ringdalen et al. (43). The nine samples from the rapid heating experiments were crushed and divided into three parallels each before they were analyzed with XRD. A Bruker D8 Focus powder diffractometer was used for all measurements. Quantitative analysis of the diffraction patterns was performed using the Bruker Topas V5 software.

3.3 Modeling of Heat Distribution in Quartz During Heating

To achieve a better understanding of the heating process of quartz in a silicon furnace, a model of heat transfer was developed in the software COMSOL Multiphysics. The heating rate used in the models was the same as in the sessile drop experiments. One model was made for a quartz cylinder of the same size and geometry as used in the sessile drop experiments, to find out if a temperature difference that might contribute to the slow melting rate, is present in the samples. In addition, models of quartz cylinders with diameter and height of 10 mm, 40 mm, 80 mm and 100 mm were developed, as these sizes are more relevant for industrial use.

36

To investigate the temperature difference, plots showing the surface temperature and temperature in the center, as a function of time, were made. The time it takes for the center to reach the same temperature as the surface, at a specific surface temperature, was found as well. 3D models of the heat distribution in the quartz were made to visualize the temperature difference. Values for the material properties specific heat capacity, thermal conductivity and density valid at 1750 °C were used as this is a temperature relevant for silicon furnaces. Specific heat capacity was obtained from Figure 2.23, thermal conductivity was found from Figure 2.22, where a constant value to 1750 °C was assumed, density was found from the software HCS 9.9. Values for the thermophysical properties are listed in Table 3.3 below.

Table 3.3 *Thermophysical data of quartz at 1750 °C.*

Property	Symbol	Value	Unit
Specific heat capacity	c_p	1250	J/K·kg
Thermal conductivity	λ	5	W/m·K
Density	ρ	2600	kg/m^3

3.4 Temperature Profile

Apparent softening and melting temperature, determined from the sessile drop experiments at a heating rate of 5,5 °C/min, were implemented to a plot of a temperature profile of a silicon furnace. This was done to examine at which depth in the furnace the quartz starts to soften and melt, and divide the furnace into different zones based on this.

4 Results

4.1 Softening and Melting Temperature of Different Quartz Types

Form the sessile drop experiments, it was observed that apparent melting temperature decrease with decreasing holding temperature, see Figure 4.1. Temperature at complete melting varied between 1730 ℃ and 1850 ℃. Softening temperature varied between 1690 ℃ and 1740 ℃. Time from beginning of experiment to complete melting varied from 72 to 130 minutes. For the experiments without holding time, quartz type A had the highest apparent melting temperature and quartz type B the lowest. Apparent softening temperature was in the same range for all parallels, but a small variation between the different quartzes was observed; B had the highest average softening temperature and C the lowest, see Figure 4.2.
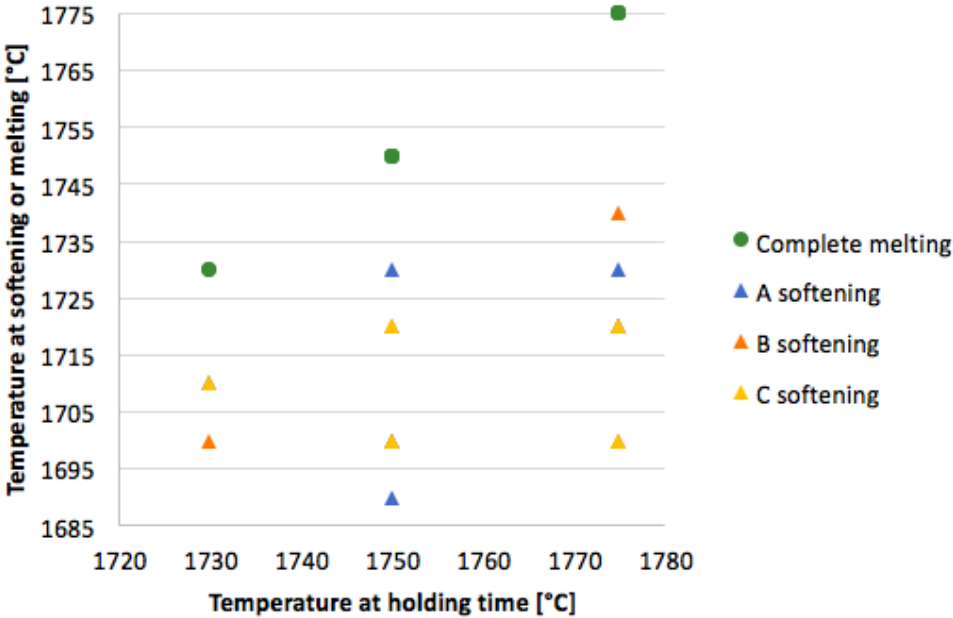

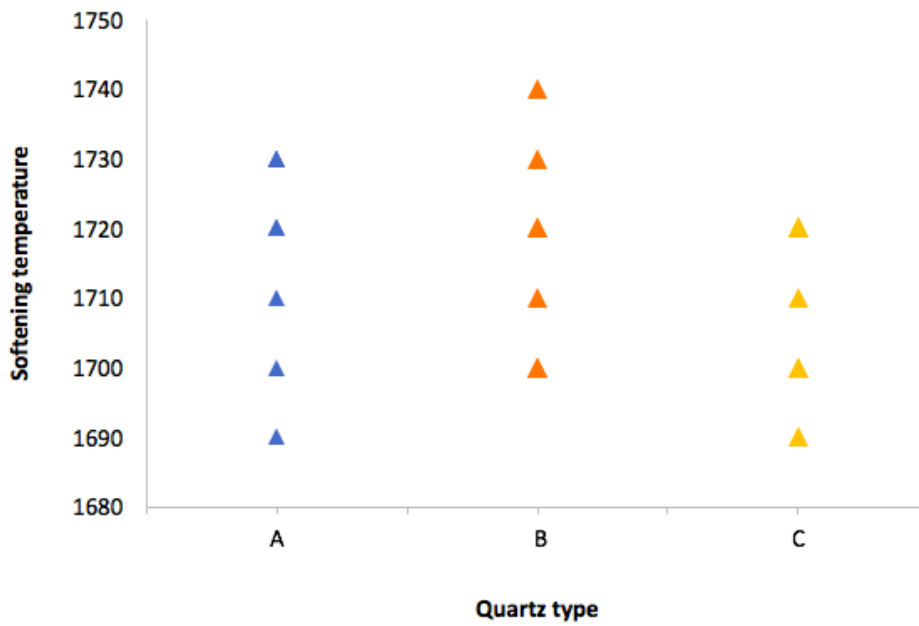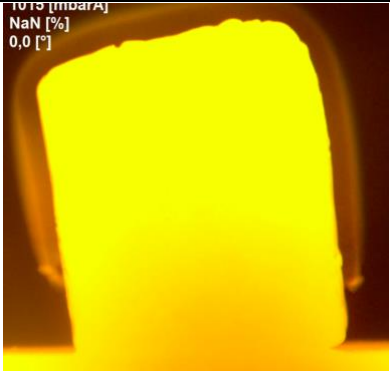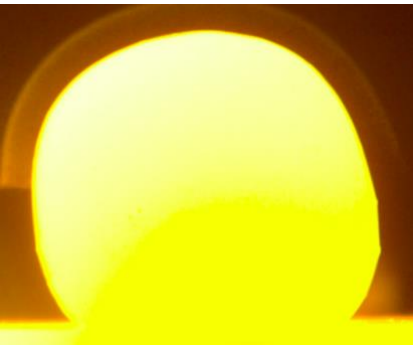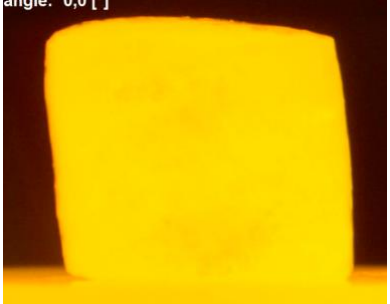***Figure 4.1*** *Apparent softening and melting temperature vs. holding temperature.*
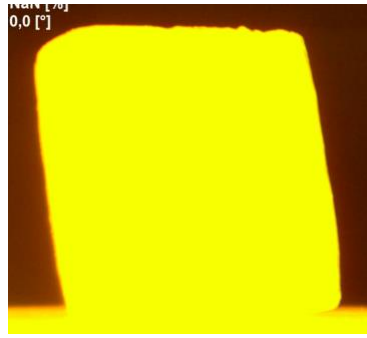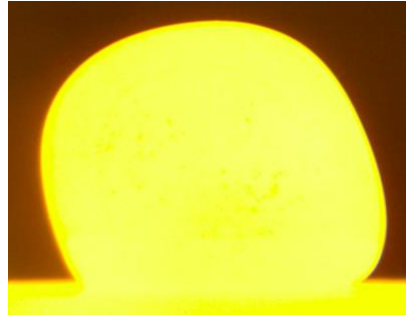
Figure 4.2 *Apparent softening temperature for three different quartz types.*

Softening temperature, temperature at complete melting, and elapsed time at complete melting, measured form the sessile drop experiments, are listed in table 4.1 below. The temperatures are rounded to the nearest 10 ℃. Images of the samples at softening and complete melting are given in table 4.2.
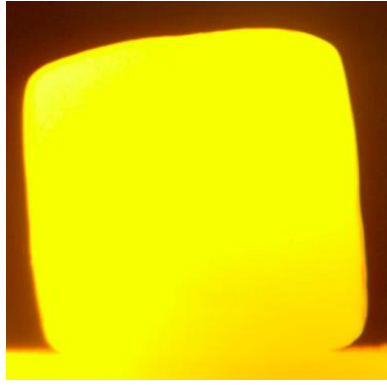
Table 4.1 *Apparent softening and melting temperature, and time at complete melting, for all parallels. Experiments where the holding time was not sufficient for melting are indicated with x.*

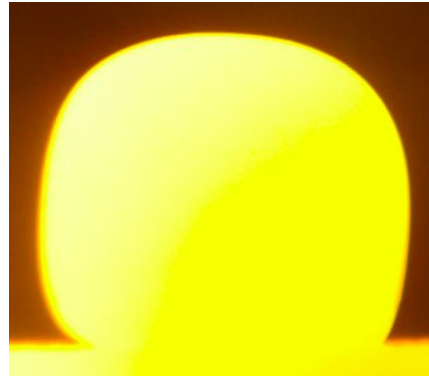| Test	Quartz type	Holding temperature [°C]	Softening temperature [°C]	Melting temperature [°C]	Time at complete melting [min]
A1	A	-	1730	1830	73
A2	A	-	1730	1850	77
A3	A	-	1720	1840	75
B1	A	1775	1720	1775	80
B2	A	1775	1730	1775	83
B3	A	1775	1720	1775	79
C1	A	1750	1690	1750	90
C2	A	1750	1730	1750	96
C3	A	1750	1700	1750	88
D1	A	1730	1710	1730	86
E1	B	-	1710	1830	73
E2	B	-	1730	1820	72
E3	B	-	1720	1800	68
F1	B	1775	1740	1775	78
F2	B	1775	1700	1775	69
G1	B	1775	1700	1775	69
G2	B	1750	1720	1750	80
H1	B	1750	1700	1750	73
I1	C	-	1720	1830	73
I2	C	-	1700	1820	71
I3	C	-	1690	1830	73
J1	C	1775	1720	1775	83
J2	C	1775	1720	1775	110
J3	C	1775	1700	1775	98
K1	C	1750	1720	1750	120
K2	C	1750	1700	1750	135
L1	C	1730	1710	x	x

Table 4.2 *Images of quartz samples in a sessile drop furnace at softening temperature and complete melting. All parallels of experiment A are given to show the variation between parallels.*

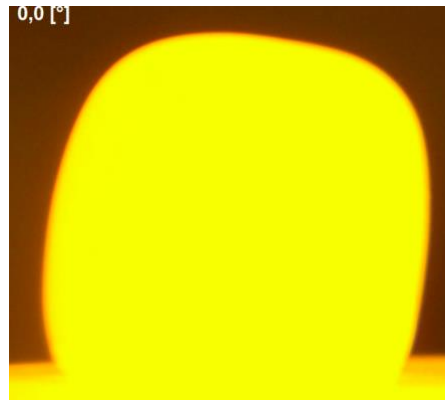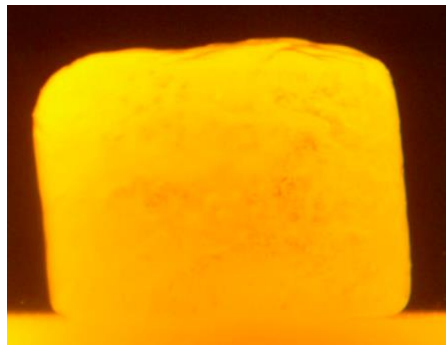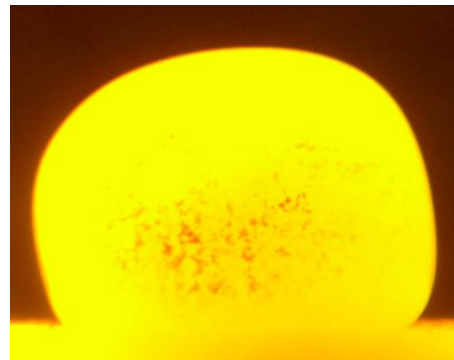| Parallel	Beginning of melting [°C]	Complete melting [°C]
A1	1730	1830
A2	1730	1850
A3	1720	1840

B1   1720   1775

C1   1690   1750

D1   1710   1730

E1   1710   1830
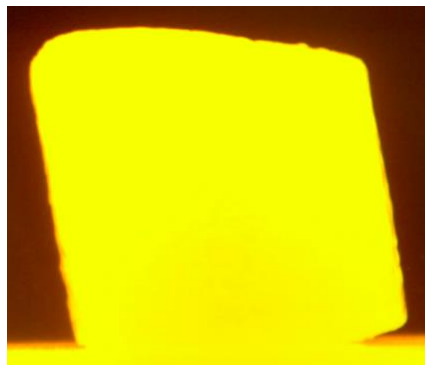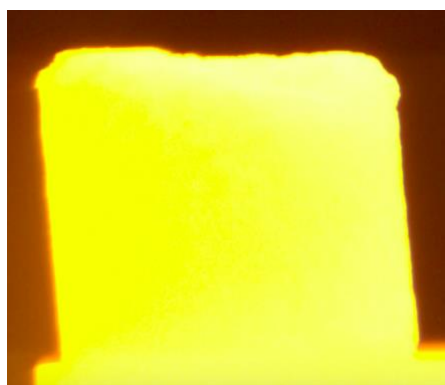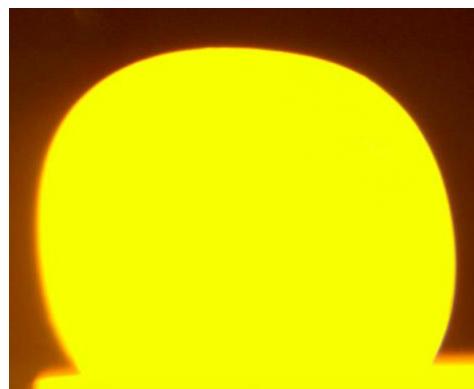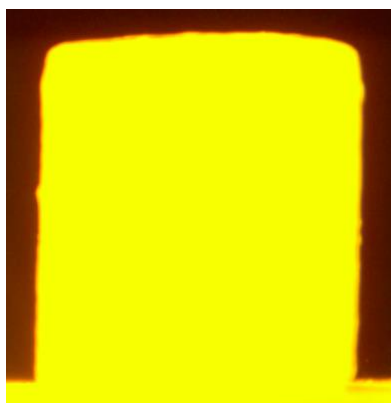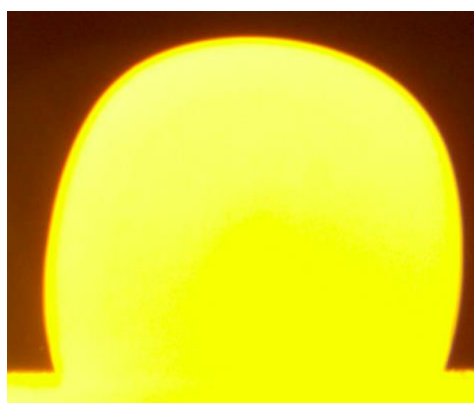
	1720	1775
F1		
	1690	1750
G1		
	1710	1730
H1		
	1710	1830
I1		

44

J1	1740 / 1775
K1	1700 / 1750
L1	1700 / X
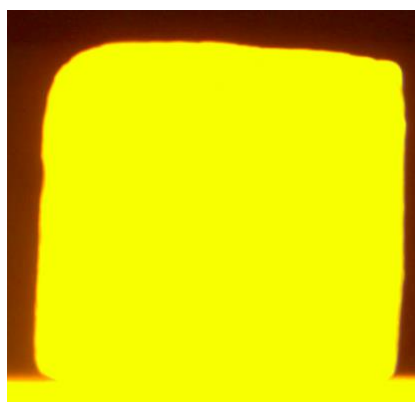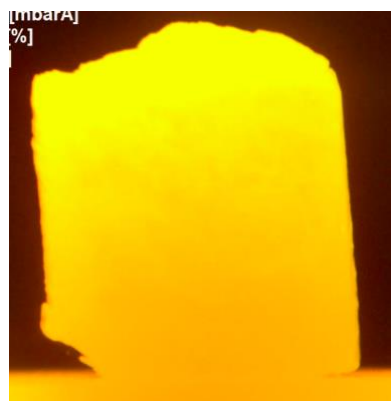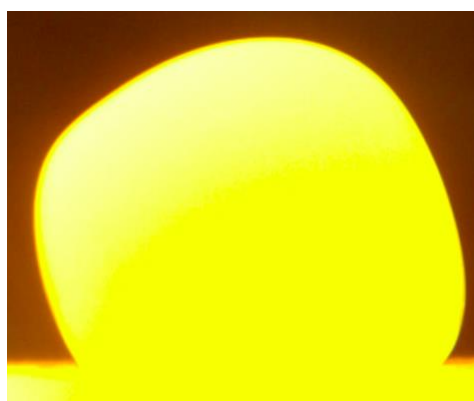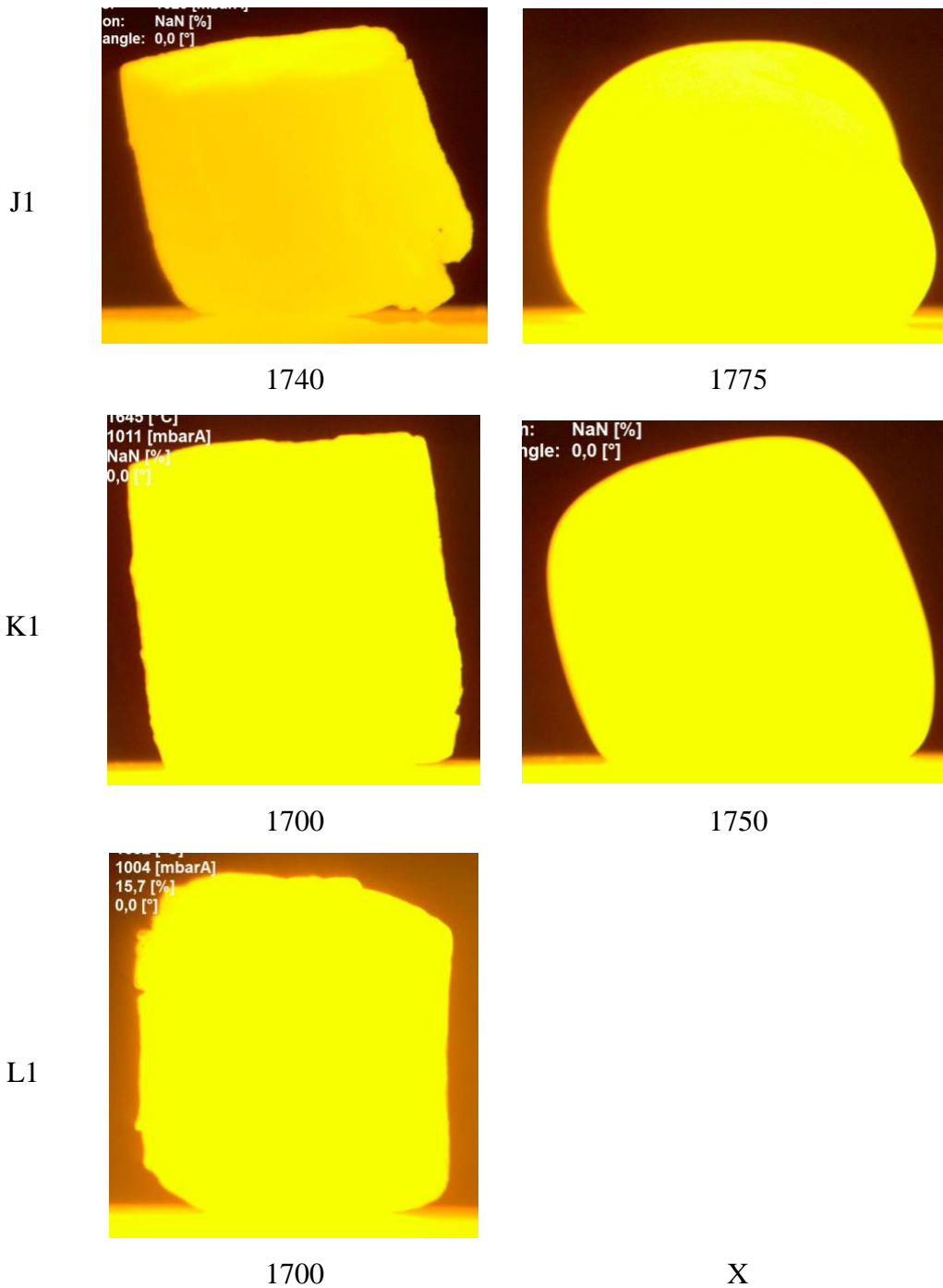
Apparent softening and melting temperature for the different heating programs used in the sessile drop furnace are marked on the graph in Figure 4.3 below. The overall trend for temperature at complete melting can be clearly seen; it decreases with decreasing temperature at holding time. It can also be observed that time before complete melting varies between the different quartzes.
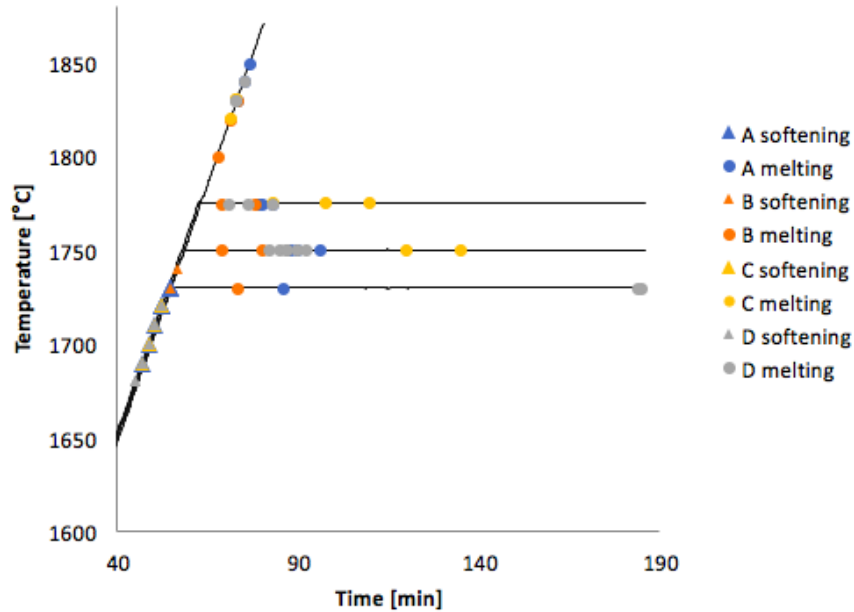
Figure 4.3 *Apparent softening and melting temperature for four different quartz types under different heating programs. The results for D are reprinted from Nordnes (20).*

4.2 Melting Kinetics

The sessile drop experiments showed that quartz has a slow melting rate, which increases with increasing temperature. This can be seen from Figure 4.3 above. A variation in melting rate between the different quartz types can be observed as well. It was found that a higher impurity content will give a higher melting rate, see Figure 4.4 below. Amount of trace elements in A is unknown, but if it follows the same linear trend as the other quartzes, the impurity concentration in A will be around 0.29 %, giving the recorded melting rate. For the experiments with holding time, the overall trend is that C had the lowest melting rate and B the highest. The same trend was seen for apparent softening temperatures between the different quartzes, presented in Figure 4.2 on page xx.
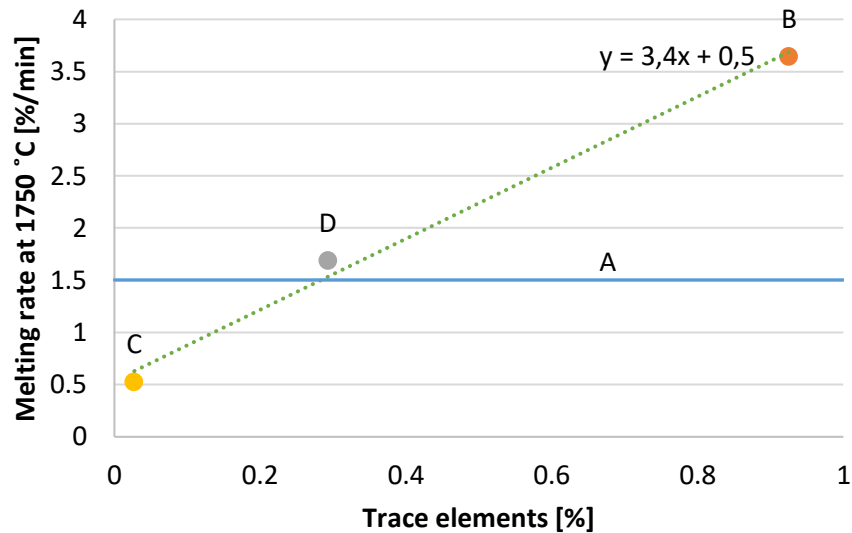
Figure 4.4 Melting rate at a holding temperature of 1750 °C as a function of trace element content. Result for D is reprinted from Nordnes (20). Values for trace element concentration are from Table 3.1. Trace element concentration for A is unknown, and therefore a line for melting rate is plotted.

Calculations of melting rate indicate the same overall trend as Figure 4.3; melting rate increase with increasing temperature. Quartz type C and B showed the lowest and highest melting rates at holding temperature, respectively. See chapter 4.2.1 for calculations. Melting rate at holding time for all parallels is listed in Table 4.3. Melting rate as a function of holding temperature is plotted in Figure 4.5, and the average melting rate for each quartz type at holding time is given in the bar graph in Figure 4.6
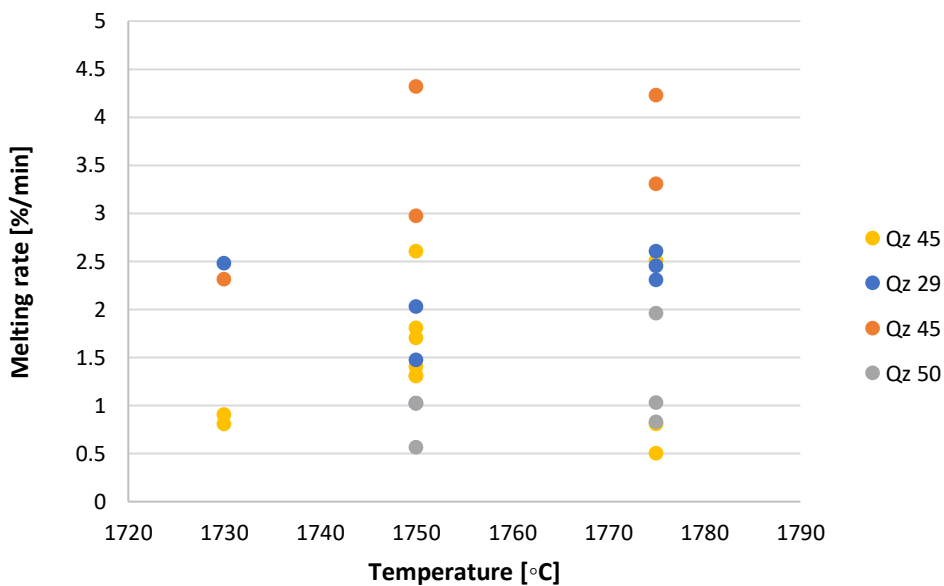
Figure 4.5 Melting rate at holding temperature. Results for D are reprinted from Nordnes (20).

47
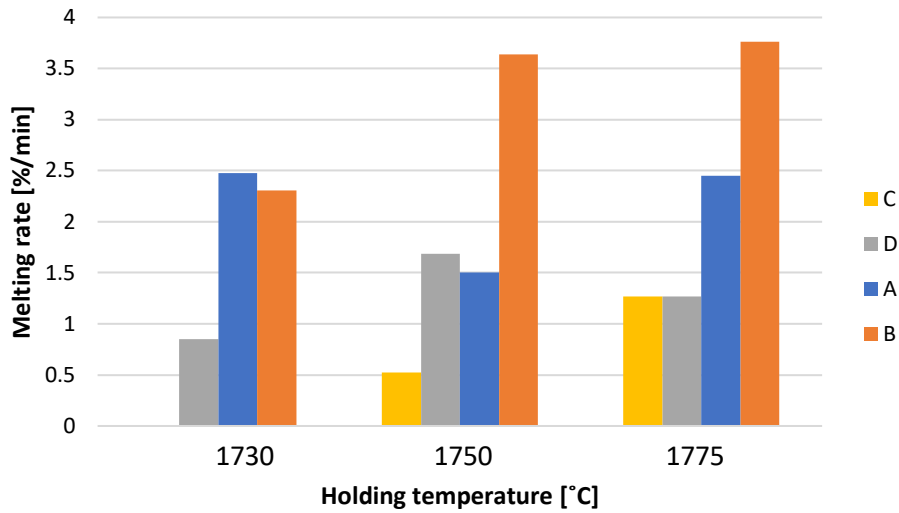
Figure 4.6 *Average melting rate at holding temperature. Results for D are reprinted from Nordnes (20).*

Table 4.3 *Melting rate at holding temperature for the different parallels.*

Parallel	Quartz type	Softening temperature [°C]	Complete melting [°C]	Melting rate at holding temperature [%/min]
B1	A	1720	1775	2.75
B2	A	1730	1775	2.90
B3	A	1720	1775	2.93
C1	A	1690	1750	1.29
C2	A	1730	1750	2.11
C3	A	1700	1750	1.71
D1	A	1710	1730	2.57
F1	B	1740	1775	4.15
F2	B	1700	1775	2.91
G1	B	1700	1775	4.14
G2	B	1720	1750	2.92
H1	B	1700	1750	2.22
J1	C	1720	1775	2.59
J2	C	1720	1775	1.09
J3	C	1700	1775	1.03
K1	C	1720	1750	1.14
K2	C	1700	1750	0.71

4.2.1 Calculations of Melting Kinetics

Melting rate, r_1, from measured softening to complete melting for the experiments without holding time can be found from

$$r_1 = \frac{x_1}{t_{m1} - t_s} = \frac{100\,\%}{\Delta t_1} = 5.5\,\%/min \qquad (4.1)$$

where $x_1 = 100\,\%$ is the amount of melted quartz from softening temperature to complete melting, Δt_1 is the time difference from time at softening temperature, t_s, to time at complete melting, t_{m1}. This equals the slope in Figure 4.7, and thus corresponds to the heating rate of 5.5 °C/min.
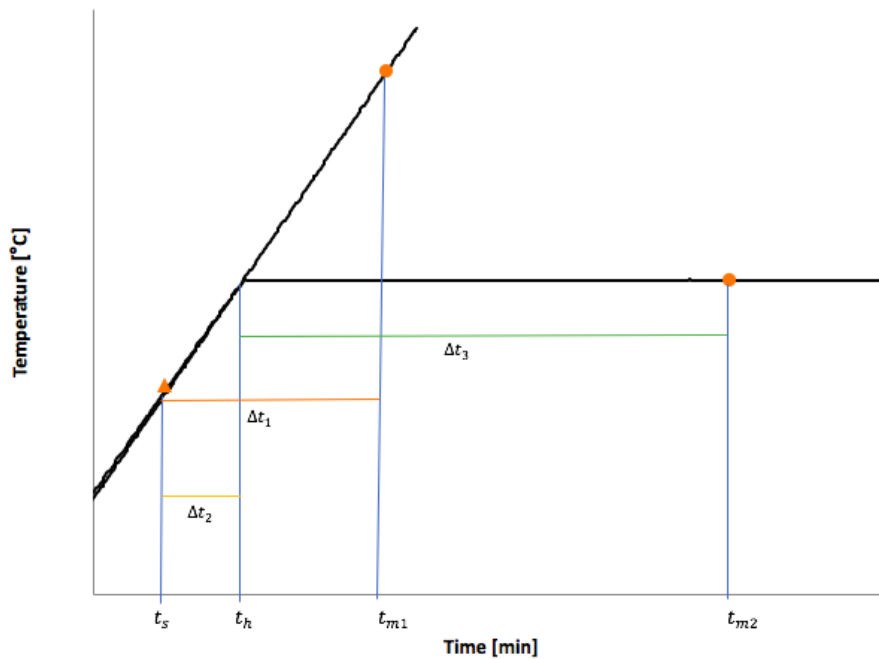
Figure 4.7 *Parameters used to calculate melting rate.*

Amount of melted sample before holding time, x_2, can be calculated from

$$x_2 = r_1 \cdot (t_h - t_s) = 5.5\,\%/min \cdot \Delta t_2 \qquad (4.2)$$

where Δt_2 is the time difference from softening temperature, t_s, to beginning of holding time, t_h, as shown in Figure 4.7.

Melting rate at holding time, r, can then be found from

$$r = \frac{x_1 - x_2}{t_{m2} - t_h} = \frac{100\,\% - x_2}{\Delta t_3} \tag{4.2}$$

where Δt_3 is the time difference between time at melting temperature at holding time, t_{m2}, as shown in Figure 4.7, and the rest of the parameters are as before.

4.3 Phase Mapping of Heat Treated Quartz

4.3.1 Visual inspection

When the samples were taken out of the rapid heating furnace and cooled, a change in color was observed. A and C had turned white and B had a light gray color. Disintegration had occurred upon heating as well. C had many cracks and was easily crumbled, A could be crumbled at the corners, whilst B showed no signs of cracking. Samples of two of the quartzes after heat treatment are shown in Figure 4.8.

(a) A after heating.   *(b) B after heating.*

Figure 4.8 *Samples of two of the quartz types used in the rapid heating experiments after heat treatment. Some disintegration can be observed.*

4.3.2 XRD Analysis

The quartzes from the rapid heating experiments were analyzed with XRD, as described by Ringdalen et al. (43). Quartz type A and C showed the highest and lowest content of amorphous phase, respectively, although some overlapping between quartz type B and C was observed. No

clear trend between melting rate and amount of amorphous phase can be seen. Weight-percent of amorphous phase as a function of average holding time at 1750 °C (recorded from the sessile drop experiments) is given in Figure 4.9.
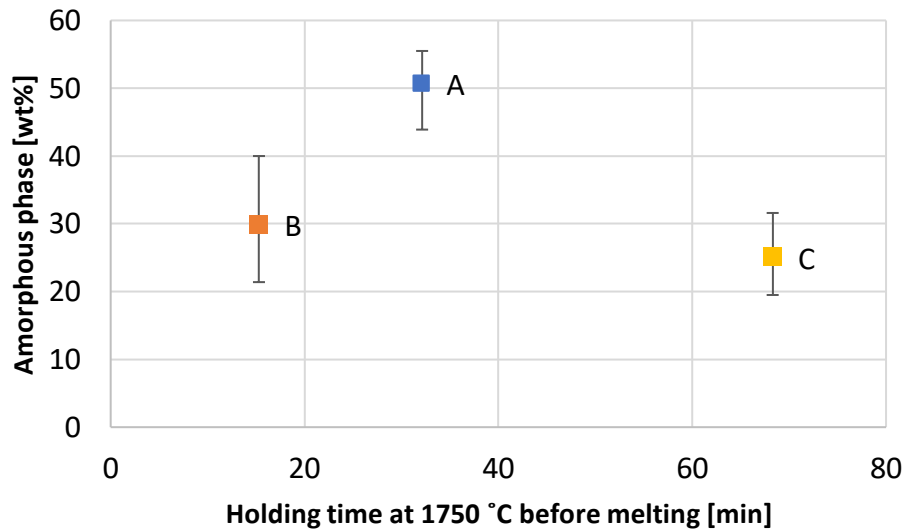
Figure 4.9 *Amount of amorphous phase after heat treatment in a rapid heating furnace to 1650 °C, for three different quartzes, as a function of average holding time at 1750 °C before complete melting in a sessile drop furnace.*

Phase distribution after heat treatment in the rapid heating furnace to 1650 °C is shown in Figure 4.10. Content of quartz, cristobalite and amorphous phase is listed in Table 4.4 below. Results for parallel C1,1-C1,3 are excluded from the plots as they deviate considerably from the other results.
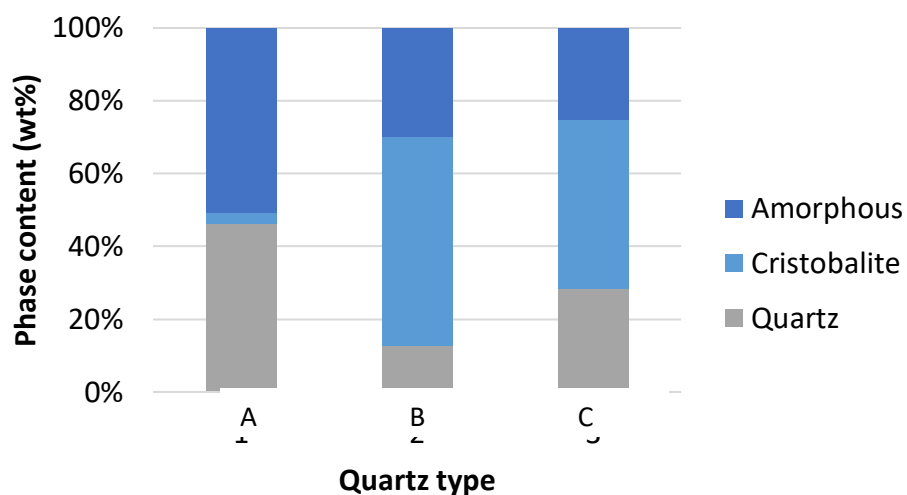
Figure 4.10 Phase distribution in three different quartzes after heat treatment to 1650 °C.

Table 4.4 Phase composition in silica after heat treatment to 1650 °C, analyzed with XRD.

Quartz type	Parallel	Quartz [wt%]	Cristobalite [wt%]	Amorphous [wt%]
A	1,1	50.8	2.8	46.4
A	1,2	53.3	2.8	43.9
A	1,3	52.6	2.8	44.6
A	2,1	44.0	3.1	52.9
A	2,2	41.3	3.2	55.5
A	2,3	39.7	3.3	57.0
A	3,1	45.1	3.8	51.0
A	3,2	44.6	3.9	51.4
A	3,3	43.2	3.9	52.8
B	1,1	12.9	55.3	31.8
B	1,2	12.6	54.3	33.1
B	1,3	13.7	61.7	24.5
B	2,1	12.1	47.9	40.0
B	2,2	12.9	48.5	38.6
B	2,3	14.0	50.5	35.5
B	3,1	12.6	65.6	21.8
B	3,2	12.4	66.0	21.7
B	3,3	11.5	67.1	21.4
C	1,1	0	90.6	9.4
C	1,2	0	87.9	12.1
C	1,3	0	89.2	10.8
C	2,1	22.4	55.7	21.9
C	2,2	22.2	58.3	19.5
C	2,3	18.5	54.7	26.8
C	3,1	35.5	36.7	27.8
C	3,2	38.5	38.7	22.8
C	3,3	32.5	35.9	31.6

4.4 Modeling of Heat Distribution in Quartz During Heating

Plots developed in COMSOL, indicate an increasing temperature difference between center and surface with increasing sample size. The plots also indicate that a slower heating rate, and a higher temperature, lead to a lower temperature difference. See Figure 4.11-4.15 for plots of surface and center temperature as a function of time for all sample sizes. Centre temperature for all sample sizes at the time when surface temperature is 1765 °C are plotted in the graph in Figure 4.16.

Figure 4.11 *Surface temperature, (2, 2) and (0, 0) and temperature in center, (0, 2) of a quartz cylinder with diameter and height of 4 mm as a function of time. A small temperature difference can be seen from the close-up to the left.*
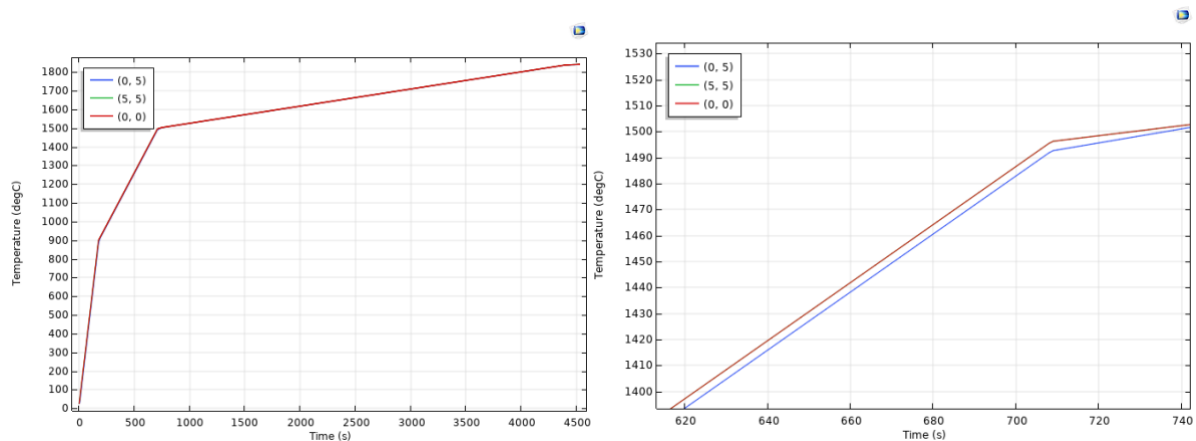
Figure 4.12 *Surface temperature, (5, 5) and (0, 0) and temperature in center, (0, 5) of a quartz cylinder with diameter and height of 10 mm as a function of time. A small temperature difference can be seen from the close-up to the left.*
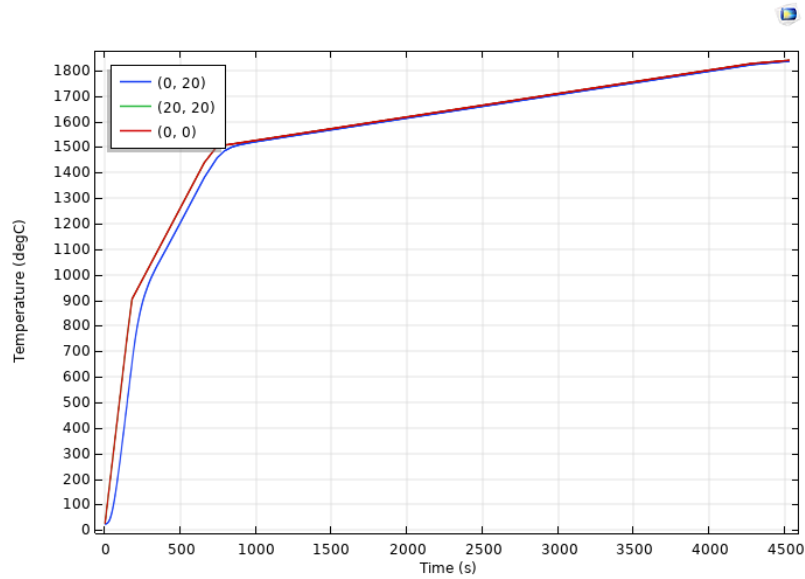
Figure 4.13 *Surface temperature, (20, 20) and (0, 0) and temperature in center, (0, 20) of a quartz cylinder with diameter and height of 40 mm as a function of time. The temperature difference decrease as the heating rate is lowered and the temperature increase.*
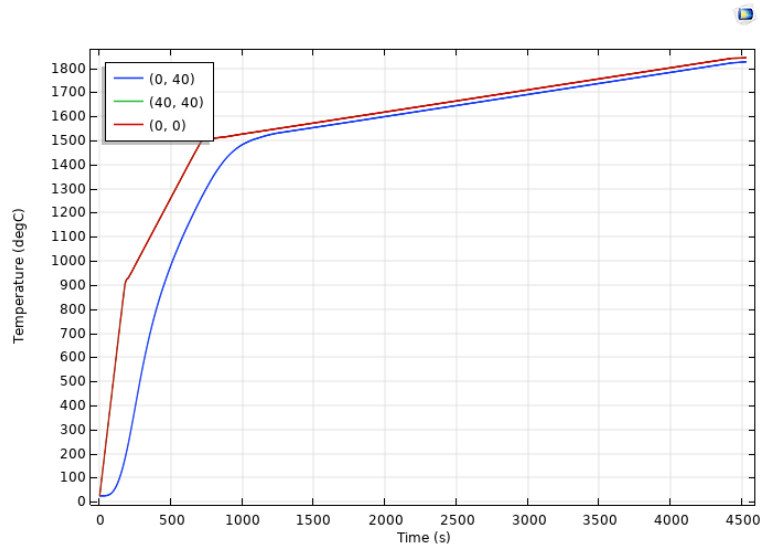
Figure 4.14 *Surface temperature, (40, 40) and (0, 0) and temperature in center, (0, 40) of a quartz cylinder with diameter and height of 80 mm as a function of time. The temperature difference seems to stabilize after some time at constant heating rate.*
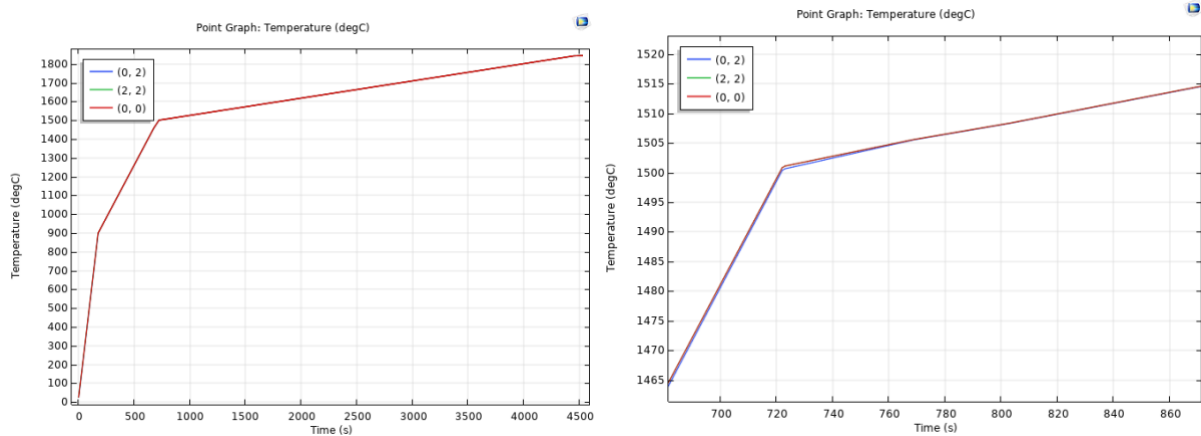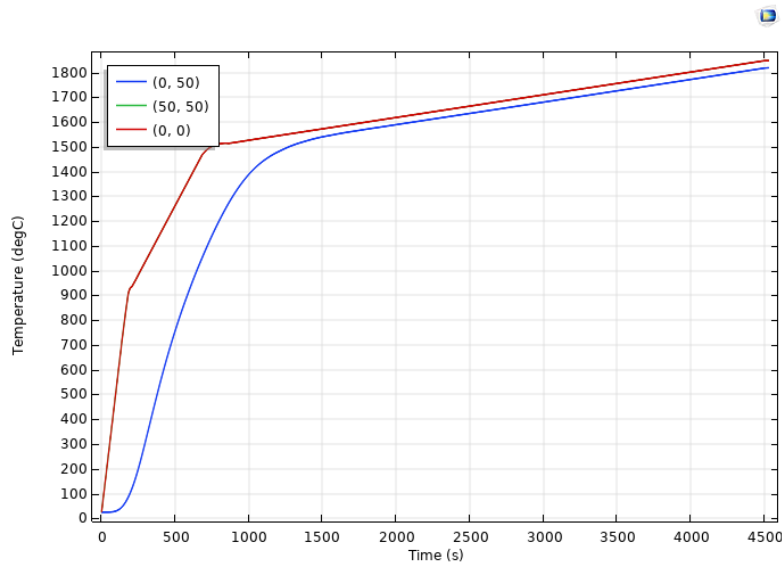
Figure 4.15 *Surface temperature, (50, 50) and (0, 0) and temperature in center, (0, 50) of a quartz cylinder with diameter and height of 100 mm as a function of time.*
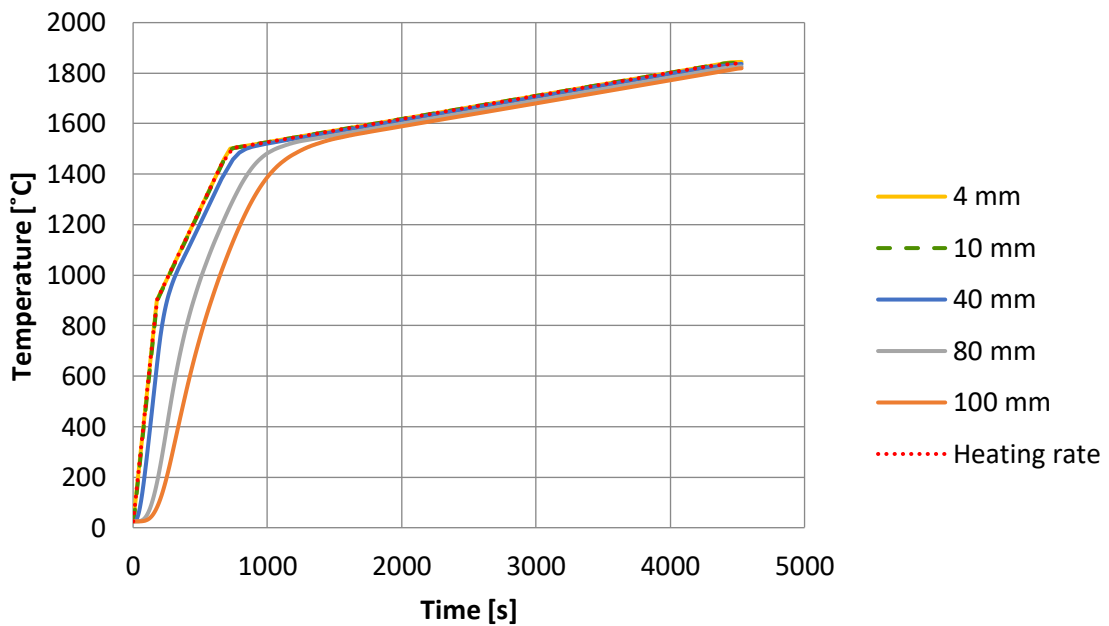
Figure 4.16 *Centre temperature in quartz cylinders of varying height and diameter at the time when surface temperature is 1765 °C.*

To visualize the temperature distribution, 3D models of the heat distribution in the quartz cylinders were made, see Figure 4.17-4.21. Just like the plots, the models indicate that larger pieces of quartz will have a larger temperature difference. Differences between surface and center varied from approximately 0.05 °C for the 4 mm sample to around 30 °C for the 100 mm sample. The models show the temperature distribution after one hour, when the surface

55

temperature was approximately 1765 °C and the heating rate was 5.5 °C/min. Different color scales are used to illustrate the variation between sample sizes.
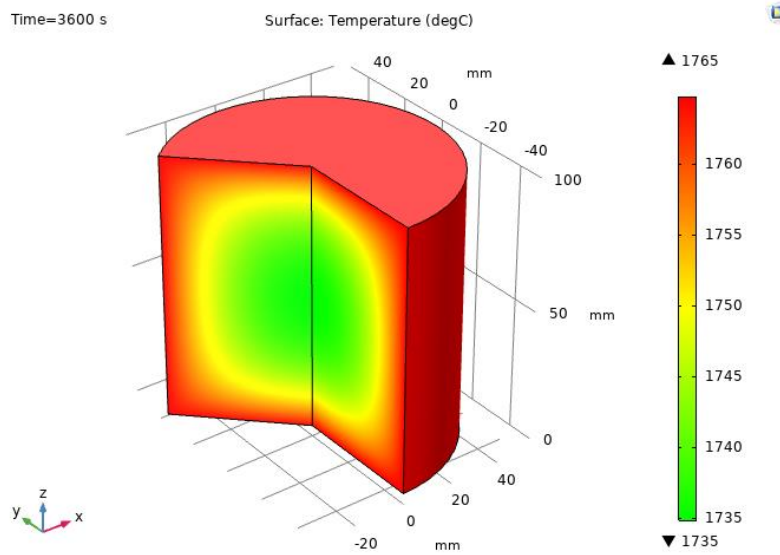
Figure 4.17 *3D model of a quartz cylinder with diameter and height of 100 mm. The figure shows a temperature difference of approximately 30 °C.*
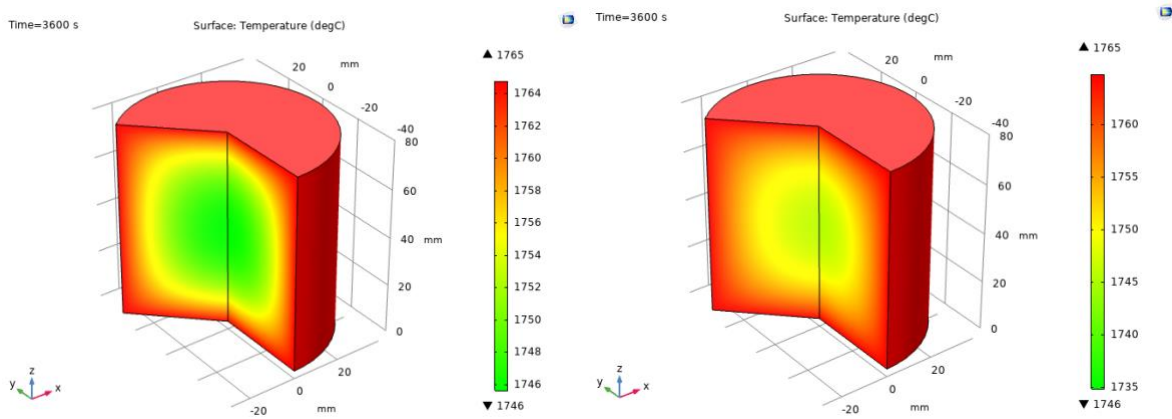
(a) The image shows a temperature difference of approximately 19 °C.

(b) The same color scale as used for the 100 mm sample is applied here.

Figure 4.18 *3D models of a quartz cylinder with diameter and height of 80 mm.*
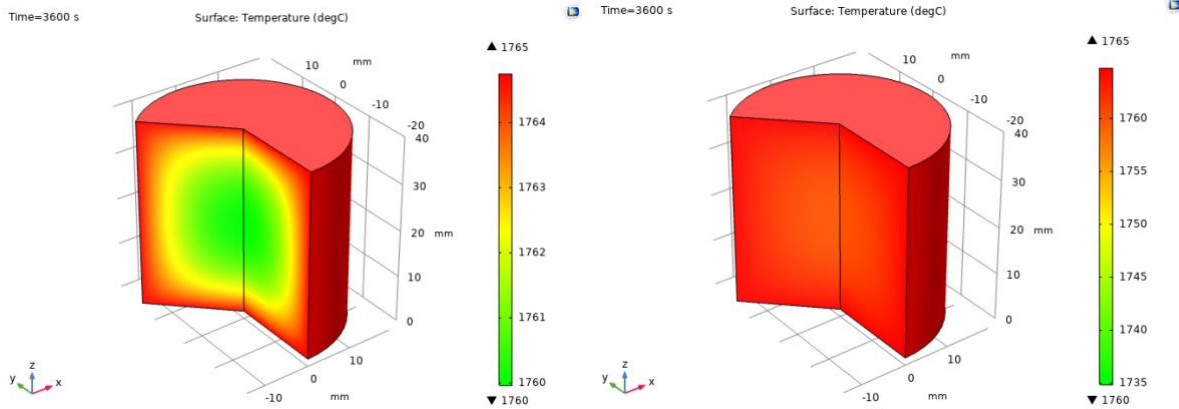
(a) The image shows a temperature difference of approximately 5 ℃.

(b) The same color scale as used for the 100 mm sample is applied here.

Figure 4.19 *3D models of a quartz cylinder with diameter and height of 40 mm.*
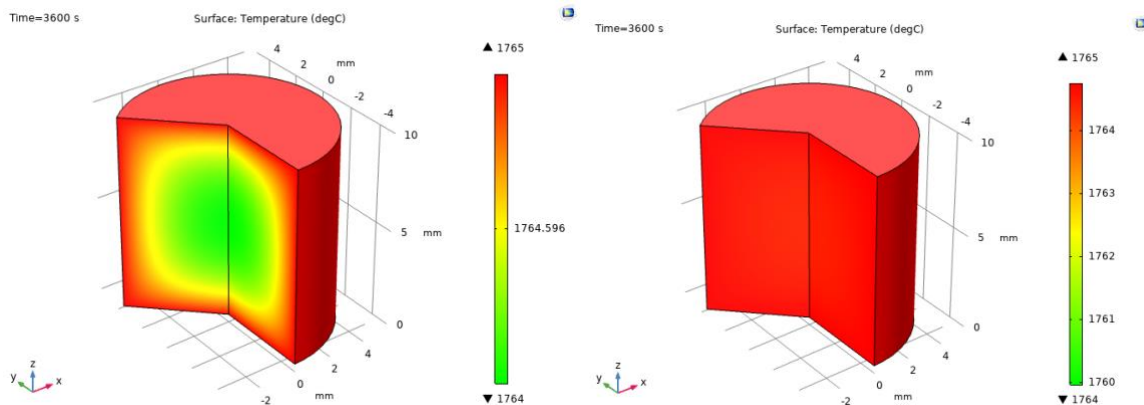
(a) The image shows a temperature difference of approximately 1 ℃.

(b) The same color scale as used for the 40 mm sample is applied here.

Figure 4.20 *3D models of a quartz cylinder with diameter and height of 10 mm.*
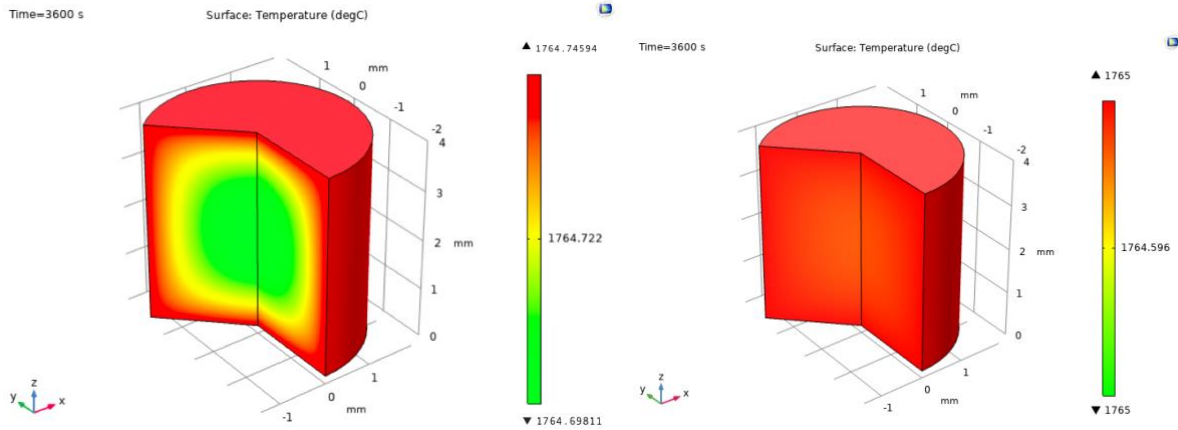
(a) The image shows a temperature difference of approximately 0,1 °C.

(b) The same color scale as used for the 10 mm sample is applied here.

Figure 4.21 *3D models of a quartz cylinder with diameter and height of 4 mm.*

The time it takes for the center to reach 1765 °C, after the surface has reached 1765 °C, was found for each quartz size, see Table 4.5. The table also includes temperature difference between surface and center. The time difference is plotted in Figure 4.22 as a function of sample size. The time difference increase with increasing quartz size.
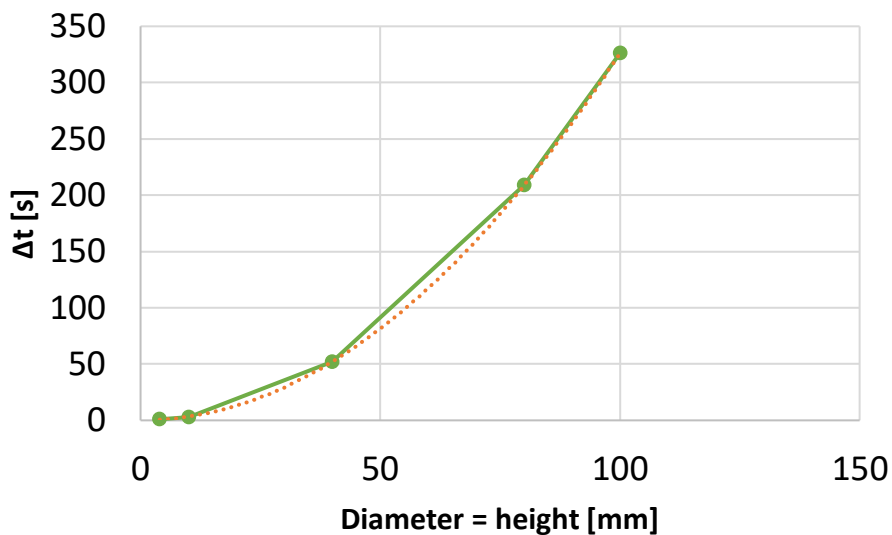
Figure 4.22 *Time it takes for the center of quartz cylinders of varying size to reach the same temperature as the surface had after one hour of heating.*

***Table 4.5** Time it takes for the center of quartz cylinders of varying size to reach the same temperature the surface had after one hour of heating, Δt, and temperature difference between surface and center after one hour, ΔT.*

Diameter=height [mm]	Surface temperature [°C]	Temperature in center [°C]	ΔT [°C]	Δt [s]
4	1764.96	1765.01	0.05	1
10	1764.96	1765.26	0.30	3
40	1764.96	1769.75	4.78	52
80	1764.96	1784.09	19.13	209
100	1764.96	1794.86	29.90	326

4.5 Temperature Profile

It was found that quartz type A will descend furthest down in the furnace before it is completely melted, and quartz type B will melt first of the three quartz types. Apparent softening temperature for the three quartzes overlapped, as shown in Figure 4.2 on page xx, and hence the furnace height where softening starts for the different quartzes will overlap. Overall, quartz type A had the smallest distance between softening and complete melting. Quartz type B was completely melted highest up in the furnace, but the distance between softening and melting was shorter than for quartz type C. Apparent softening and melting temperature from the sessile drop experiments are indicated on the temperature profile given in Figure 4.23 below. Average depth at apparent softening and melting temperature, and distance between softening and melting, for the three quartzes are listed in Table 4.6.
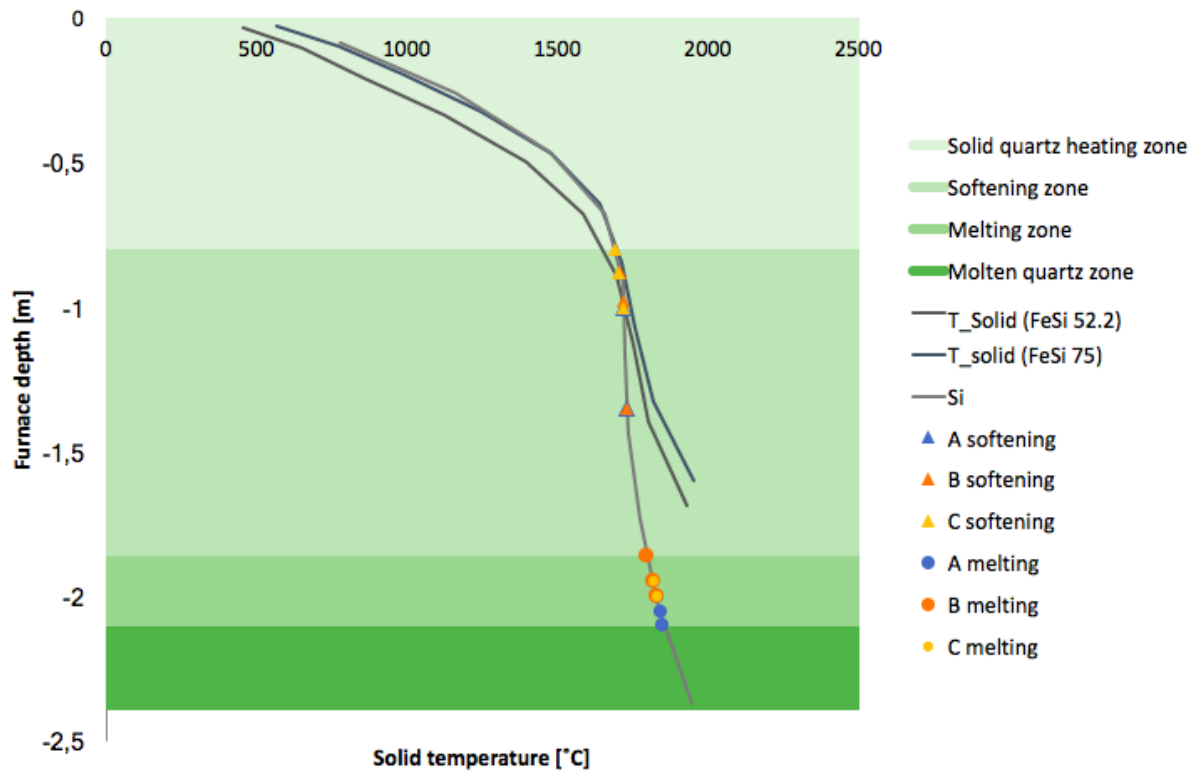
Figure 4.23 *Temperature profile for solids in a production furnace, supplied by Elkem (44). Apparent softening and melting temperature from the sessile drop experiments are marked on the graph for silicon.*

Table 4.6 *Melting process in a silicon furnace for different quartzes.*

Quartz type	Average depth at softening [m]	Average depth at melting [m]	Average distance between softening and melting [m]	Furnace containing molten quartz [%]
A	-1.23	-2.05	0.82	13.05
B	-1.08	-1.94	0.86	18.29
C	-0.89	-1.98	1.09	16.32

Further, the furnace was divided into four different zones based on apparent melting and softening temperature. From top to bottom they might be called solid quartz heating zone, softening zone, quartz melting zone and molten quartz zone. The different zones are given in Table 4.7, and are indicated with different shades in the background in Figure 4.23.

Table 5.1 Zones in a silicon production furnace.

Zone	Distance from charge top [m]
Solid quartz heating zone	0 to 0.8
Softening zone	0.8 to 1.9
Melting zone	1.9 to 2.1
Molten quartz zone	2.1 to 2.4

5 Discussion

5.1 Effect of Different Parameters on Melting Properties of Quartz

Apparent melting temperature of quartz, recorded from sessile drop experiments, were higher than the theoretical melting temperature of 1713 °C (15), and it decreased with decreasing holding temperature, see Figure 5.1. From the same figure, it can also be observed that the measured melting temperatures were highest for the tests without holding time, where a heating rate of 5.5 °C/min was used from 1500 °C until complete melting. The same results were obtained from a previous study by Nordnes (20). The observations also supports the results from investigations by Ringdalen et al. (1), where it was suggested that softening and melting temperature increase with increasing heating rate.

Figure 5.1 *Apparent softening and melting temperature for four different quartz types under different heating programs in a sessile drop furnace. The results for D are reprinted from Nordnes (20).*

Quartz can sustain a high superheating, and has a high viscosity (33). The high viscosity can make the quartz behave nearly as a solid at the melting temperature, and the shape of the samples will be unchanged for some time after melting temperature is reached. Thus, it can be difficult to tell when a sample is melted from visual inspection of the recorded video of the melti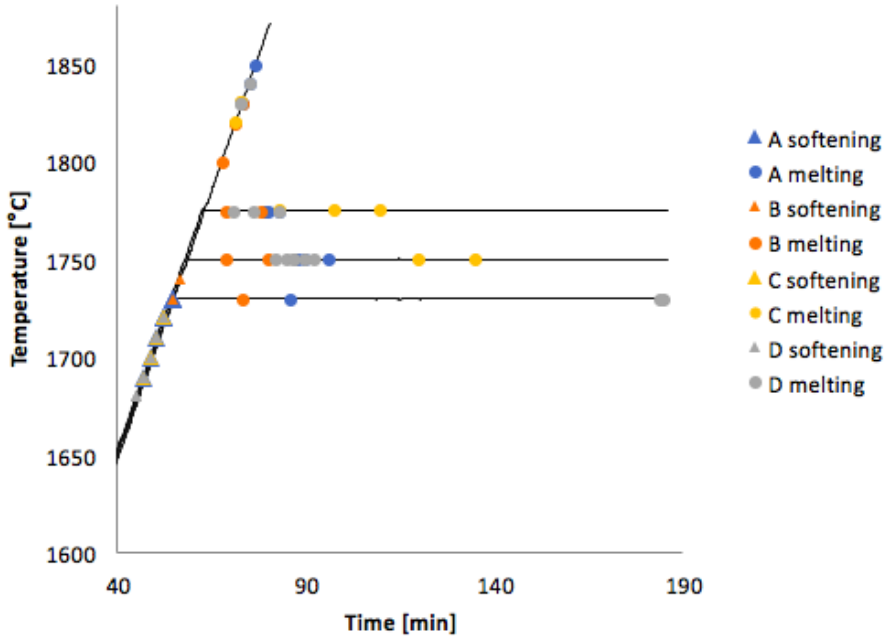ng process in the sessile drop furnace. Structural changes within the samples, that cannot be seen from the video, might take place before the shape is rounded. Therefore, viscosity might have a large impact on the measured softening and melting temperatures.

According to the Alkemade theorem, impurities will lower the melting point of a substance (29). As discussed, the recorded melting temperatures were higher than the theoretical for all three quartz types. This indicates that the high viscosity has a larger effect on melting behavior than the relatively low impurity concentration. However, the measured melting rates did, in fact, decrease with increasing level of impurities, as expected from the Alkemade theorem.

5.2 Mechanism and Kinetics of Melting

It was observed that the closer the temperature at holding time was to the theoretical melting temperature, the longer time it took for the samples to melt, i.e. melting rate increase with increasing temperature. This is expected as the temperature difference between theoretical melting temperature and apparent melting temperature is the driving force for the melting process (35), and the viscosity decrease with increasing temperature (1).

From the sessile drop experiments, an overall trend for melting rate between the different quartz types was observed as well; quartz type B, which have the highest concentration of impurities, had the highest melting rate, and C, which have the lowest concentration of impurities, the lowest melting rate. This effect of trace elements is expected, since an increase in trace elements will both lower the melting point (29) and the viscosity (33) , and hence increase the observed melting rate. Calculations of melting rate showed a relatively linear increase as a function of impurity concentration, after the function $y = 3.4x + 0.5$, where y is melting rate and x is impurity concentration.

Calculated melting rates for some of the parallels deviates from the overall trend. Quartz type A showed a particularly high melting rate at 1730 °C (parallel D1), compared to the other results. From inspections of the recorded video from the sessile drop furnace, it was observed

that smaller samples seemed to have a higher melting rate than larger samples of the same type under the same temperature conditions. This accounts for parallel D1, which was a relatively small sample. Thus, the melting rate can be considered to be lower for a sample with a height of 4 mm, and thus the overall trend of increasing melting rate with increasing holding temperature seems to be fulfilled for quartz type A. Quartz type C (from parallel L1) did not melt even after 180 minutes at a holding temperature of 1730 °C, and the melting rate is thus below 0.5 %/min. This indicates that the trend for C is complete as well.

The detected phase composition from the XRD analysis showed no correlation between amount of amorphous silica and melting rate for the different quartzes. Quartz type C contained the lowest amount of amorphous phase and had the lowest melting rate, while B, which had the highest melting rate, contained around half as much amorphous silica as quartz type A. Amount of amorphous phase for all parallels is given in Figure 5.2. No correlation between melting rate and amount of quartz or cristobalite was seen either.

For a sample to melt completely, it must be heated to the center. 3D models and plots developed in COMSOL showed an increase in temperature difference between surface and center with increasing sample size. For cylindrical quartz samples with diameter and height of 4 mm, as used in the sessile drop furnace, a small temperature difference of around 0.05 °C between surface and center was measured at a surface temperature of 1765 °C. The same heating program, without holding time and a heating rate of 5.5 °C/min, as used in the sessile drop furnace, was used. A center temperature of 1765 °C will be reached after 1 second. This indicates that heat transfer is not the time-limiting factor leading to the low melting kinetics. Models by both Kjeldstadli (18) and Ksiazek (40) indicate the same results as this work, and hence support the assumption that viscosity might be the main property leading to the slow melting rate and high apparent melting temperature. For larger industrial sized samples, on the other hand, heat conduction might be slowing down the melting process, as it takes longer time for the quartz to be heated to the center. According to the models, the temperature difference is approximately 30 °C, and the center will reach 1765 °C after 326 seconds, for a cylinder with height and diameter of 100 mm.

It was observed that disintegration occurred upon heat treatment in the rapid heating furnace. The fact that the samples of quartz type C was easily crumbled, supports investigations by Wiik

(19) and Nordnes (20), suggesting that the phase transformation follows the mechanism homogeneous nucleation. Quartz type A could only be crumbled at the corners, while B showed no signs of cracking. This indicates that disintegration decrease with increasing impurity concentration. A variation in disintegration between different quartz sources was observed in previous investigations by Jusnes et al. (9), as well.

5.3 Effect of Different Quartz Properties on Furnace Behavior

After heat treatment in a rapid heating furnace, quartz type C showed the highest level of disintegration and B the lowest. This means that C might produce the most fines that will reduce the charge permeability, and increase the reaction area and reaction rates in the low temperature zone, the most, and thus have the most negative effect on furnace operation. However, properties such as melting behavior and volume expansion should also be taken into account.

Implementation of apparent softening and melting temperature, recorded from the sessile drop experiments, to a temperature profile of a silicon production furnace, was used to divide the furnace into the four zones solid quartz heating zone, softening zone, melting zone and molten quartz zone, as presented in Table 5.1. The table indicates a relatively large softening zone, which can have a negative effect on the production furnace operations. The large zone might correspond to the low melting rate, discussed earlier.

Table 5.1 *Zones in a silicon production furnace.*

Zone	Distance from charge top [m]
Solid quartz heating zone	0 - 0.8
Softening zone	0.8 - 1.9
Melting zone	1.9 - 2.1
Molten quartz zone	2.1 - 2.4

It was found that quartz type A will soften and melt furthest down in the furnace. It was also observed that the distance between softening and melting was shortest for A, although softening and melting zones for the different quartzes overlapped. According to these findings, it can be expected that quartz type A will be a good choice to minimize number of particles from gluing together, and thus decrease charge permeability (5). Softening high up in the furnace is undesirable, as it might have a negative effect on reaction rates, as well (9).

5.4 Uncertainties and Accuracy of Method

5.4.1 Sessile Drop Furnace

Temperature calibration test of the type C thermocouple in the sessile drop furnace showed a calibration of -31 °C after 70 tests in Ar (42). This indicates that the recorded temperatures might have a significant impact on the results, depending on how often the thermocouple is calibrated, given the relatively small temperature differences form the experiments. The pyrometer in the furnace measured different temperatures than the thermocouple, and the difference increased as the furnace temperature increased (23). Thus, the uncertainty increase as holding temperature increase. Apparent melting temperature for the tests without holding time showed a different trend than the tests with holding time. This might be due to the uncertainty in the measurements.

The sample preparation was done using a cutting pliers, on cylinders with diameter of 4 mm drilled from larger lumps, to make the height approximately 4 mm. This was difficult as the quartz tended to crack, and thus the height of the samples varied. Inspections of the recorded videos from the sessile drop furnace showed that smaller samples had a higher melting rate than larger samples of the same quartz type under the same holding temperature, i.e. sample size affects the melting rate.

The quartz samples were drilled form different lumps. Quartz is an inhomogeneous material, meaning that the level of trace elements will vary between samples of the same quartz type. According to Stølen and Grande (28) melting temperature varies with concentration of impurities. This means that it is expected to find different softening and melting temperature for different samples, not only between different quartz types, but also for samples of the same type. However, it is not known how large the variations are expected to be.

The samples were drilled in different directions from the lumps as well, and thus the crystallographic directions within the samples will vary. Since quartz is an anisotropic material (13), this can affect the observed melting behavior.

Measured softening temperature is expected to be the same for all parallels of the same quartz type. Images were recorded every 10th second, giving a temperature increase of 0.9 °C for every new picture when the heating rate was 5.5 °C/min. The measured temperature was rounded to

the nearest 10 °C. However, there was 50 °C between the highest and lowest measured softening temperature. It was also observed that elapsed time at complete melting for different parallels of the same quartz type at the same holding temperature varied as well. This might indicate that the samples can have different levels of impurities, and that the measuring method with visual inspection of the recorded video is not precise.

5.4.2 Rapid Heating Furnace

Sample preparation for the rapid heating experiments was done using a hammer on larger lumps. This method made it difficult to make samples of the exact same weight and geometry. The models made in COMSOL showed that it takes longer time for larger sample sizes to be heated to the center, and this might affect the melting process and the phase formation.

Jusnes (45) compared the furnace thermocouple with an additional thermocouple. She found that when the furnace was heated to 1600 °C, the additional thermocouple showed an average temperature of 1615 °C after five tests. When the furnace was heated to 1700 °C, the thermocouple showed around 1705 °C for three tests. This indicates that the samples were heated to a temperature a little higher than 1650 °C, but the effect on phase composition is expected to be small.

5.4.3 XRD Analysis

The XRD analysis showed uncertainty in both method and sampling. In Figure 5.2, represents the variation between the different shades for each quartz type the uncertainty in sampling, and the variation between the bars of the same shade the uncertainty in method. Average amount amorphous phase with standard deviation is 50.6±4.4 wt%, 29.8±7.1 wt% and 25.1±3.3 wt% for quartz type A, B and C, respectively.
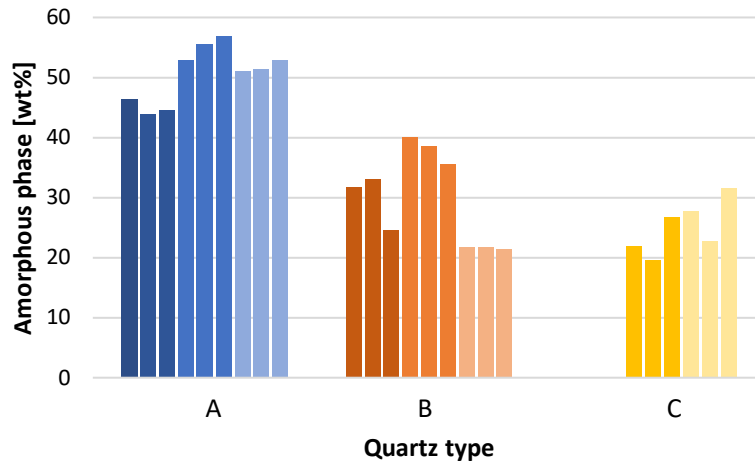
Figure 5.2 *Weight percent of amorphous silica for three quartz types detected with XRD.*

5.4.4 Temperature Profile

Assumptions made for the temperature profile are a constant quartz concentration, and a heating rate of 5.5 °C/min, throughout the furnace, that the temperature profile is correct, and correct apparent softening and melting temperatures. From the profile, it can be observed that the heating rate is not constant. As discussed, apparent softening and melting temperature have a considerably uncertainty, and it is not likely that the concentration of quartz will be constant throughout the furnace. Thus, the division of the different zones can be considered an approximation to a real furnace.

6 Conclusion

A total of 27 experiments of three different quartz types were carried out in a sessile drop furnace. Apparent softening and melting temperature indicate that quartz has a slow melting rate, that increase with increasing impurity concentration and temperature. All recorded melting temperatures were higher than the theoretical melting temperature of pure quartz, and decreased with decreasing holding temperature. The tests with a heating rate of 5.5 °C/min, showed the highest apparent melting temperatures. This indicates an increase in melting temperature with increasing heating rate.

To investigate if a slow heat transfer contributes to the high apparent softening and melting temperatures and low melting rates, models of heat conduction in quartz were developed in the software COMSOL. It was found that the sample size used in the sessile drop experiments will be heated to the center after around 1 second at 1765 °C. This indicates that heat transfer is negligible when it comes to melting rate for the small samples used in the sessile drop experiments. However, larger industry sized particles showed a longer time to be heated to the center, and hence heat transfer might slow down the melting process.

The high viscosity and superheating of quartz might make the shape of the quartz samples unchanged for a longer time after melting temperature is reached. Thus, the high viscosity seems to be an important property leading to the high apparent softening and melting temperatures and low melting rates.

Quartz samples with masses of 15±5 g were heat treated to 1650 °C in a rapid heating furnace, and analyzed with XRD. The XRD analysis failed to show any correlation between phase composition and melting rate, impurity concentration or disintegration.

Apparent softening and melting temperature from the sessile drop experiments were used to divide a temperature profile of a silicon production furnace into four different zones, based on the melting process of quartz as it descends. It was observed that the softening zone is relatively

large. This might correspond to the slow melting rate of quartz. The different quartzes started to soften and melt at different depths in the furnace, although they overlapped. Several assumptions were made to determine the different zones, and thus it can be considered an approximation of a real furnace.

Further, it could be interesting to calculate the activation energy for the melting process from kinetics data. To do this, it is necessary to know the melting mechanism. Other ways to calculate the melting rate could be to find the time difference between theoretical melting temperature and complete melting or softening temperature and complete melting, and compare these to the total time at complete melting. Effect of different atmospheres, holding times, heating rates and temperatures are also relevant parameters to examine to achieve the information needed to calculate the activation energy.

Bibliography

1.   Ringdalen E, Tangstad M. Softening and Melting of SiO2, an Important Parameter for Reactions With Quartz in Si-Production.
2.   Wu G, Yazhenskikh E, Hack K, Wosch E, Muller M. Fuel Processing Technology2015.
3.   Tangstad M. Metal Production in Norway. Oslo: Akademika; 2013.
4.   Kero I, Grådahl S, Tranell G. Airborne emissions from Si/FeSi production. 2017.
5.   Schei A, Tuset J, Tveit H. Production of high silicon alloys. Trondheim: Tapir; 1998.
6.   Ringdalen E, Tangstad M. Reaction Mechanisms in Carbothermic Production of Silicon, Study of Selected Reactions. 2012.
7.   Ringdalen E, Adisty D, Kolbeinsen L. Changes in Quartz During Heating and the Possible Effects on Si Production. 2014.
8.   Ringdalen E, Adisty D, Kolbeinsen L. Quartz-cristobalite transformation and its effect on reactions in si production: Initial studies. 2014:225-36.
9.   Ringdalen E, Tangstad M, Jusnes KF. Shock Heating of Quartz used in Silicon and Ferrosilicon Production. 2018.
10.   Bakken FO, Paulsen CO. Thermal stability of quartz for silicon process. 2013.
11.   Edfelt H, Nordnes E. Permeability Tests of Packed Bed in the Silicon Production Process. Student report, NTNU. 2018.
12.   Ringdalen E. Quartz properties in the silicon production. Silicon for the Chemical and Solar Industry XII. 2014.
13.   Callister WD, Rethwisch DG. Materials Science and Engineering. 8th ed: John Wiley & Sons; 2011.
14.   Aasly K. Properties and behavior of quartz for the silicon process. 2008.
15.   Alyward G, Findley T. SI Chemical Data. 6th ed: Wiley; 2008.
16.   Stevens SJ, Hand RJ, Sharp JH. Polymorphism of silica. Journal of Materials Science. 1997.
17.   MacKenzie JD. Fusion of Quartz and Cristobalite Research Laboratory, General Electric Company, Schenectody, New York
18.   Kjelstadli ME. Kinetics and Mechanism of Phase Transfor- mation from Quartz to Cristobalite. Student report, NTNU. 2016.
19.   Wiik K. Kinetics of Reactions Between Silica and Carbon 1990.
20.   Nordnes E. Softening and Melting Properties of Quartz. Student report, NTNU. 2018.
21.   Raz U, Girsperger S, Thompson AB. Thermal expansion, compressibility and volumetric changes of quartz obtained by single crystal dilatometry to 700°C and 3.5 kilobars (0.35 GPa).
22.   Salmang H, Scholze H. Keramik. 1982.
23.   Fjelstad Jusnes K. Parameters Affecting Softening and Melting of Quartz. Student report, NTNU. 2016.
24.   Zumdahl SS. Chemical Principles. 6 ed: Houghton Mifflin; 2009.

25.   Helbæk M, Kjelstrup S. Fysikalsk kjemi. 2 ed: Fagbokforlaget Vigmostad & Bjørke AS; 2009.

26.   Seltveit A. Refractories. Trondheim: Tapir Forlag; 1992.

27.   Kallfelz PL. Quartz for Production of Silicon Metal - Criteria for the Right Choice. Internal report Elkem ASA, Silicon Division.

28.   Stølen S, Grande T. Chemical Thermodynamics of Materials: Macroscopic and Microscopic Aspects.: John Wiley & Sons; 2004.

29.   Malakhov DV. A rigorous proof of the Alkemade theorem
. 2004.

30.   Elkem. Chemical analysis supplied by Elkem.

31.   Andersen V. Investigation of thermal properties of quartz for the silicon industry under reducing atmosphere. Student report, NTNU. 2009.

32.   Karthika S, Radhakrishnan TK, Kalaichelvi P. A Review of Classical and Nonclassical Nucleation Theories. Department of Chemical Engineering, National Institute of Technology, Tiruchirappalli. 2016.

33.   Ainslie NG, Mackenzie JD, Turnbull D. Melting Kinetics of Quartz and Cristobalite. Journal of Physical Chemistry. 1961.

34.   Hayes P. Chemical Reaction Kinetics. School of Chemical Engineering, The University of Queensland, Queensland, Brisbane, Australia.

35.   Fogler HS. Essentials of Chemical Reaction Engineering Pearson Education, Inc.; 2011.

36.   Bird RB, Stewart WE, Lightfoot EN. Transport phenomena. 2 ed. USA: John Wiley & Sons; 2002.

37.   Geankoplis CJ. Transport Processes and Separation Process Principles. 4 ed. USA: Prentice Hall; 2008.

38.   Książek M. The thermophysical properties of raw materials for ferromanganese production. 2012.

39.   Car R, Scandolo S, Srolovitz DJ, Yoon Y-G. Thermal conductivity of crystalline quartz from classical simulations. 2004.

40.   Ksiazek M. Heat transfer in quartz particle – modelling in Comsol Multiphysics. 2017.

41.   West AR. Basic Solid State Chemistry1999.

42.   Bao S. Temperature calibration of type C thermocouple in furnace 1, wetting lab. 2019.

43.   Ringdalen E, Tolchard J, Thonassen E. Evaluation of methods used to measure amount of phases in silica. SINTEF Materials and Chemistry. 2017.

44.   Hammervold A, Cybernetica, University E. Simulated temperature profiles using FeSiMod. Elkem's proprietary dynamic simulation model for the FeSi/Si process. 2017.

45.   Personal communication with Karin Fjeldstad Jusnes. 2019.